Ground state properties and response functions in DFT

Carlos Bertulani
Department of Physics and Astronomy
Texas A&M University-Commerce

From 100 to 10^{57} nucleons

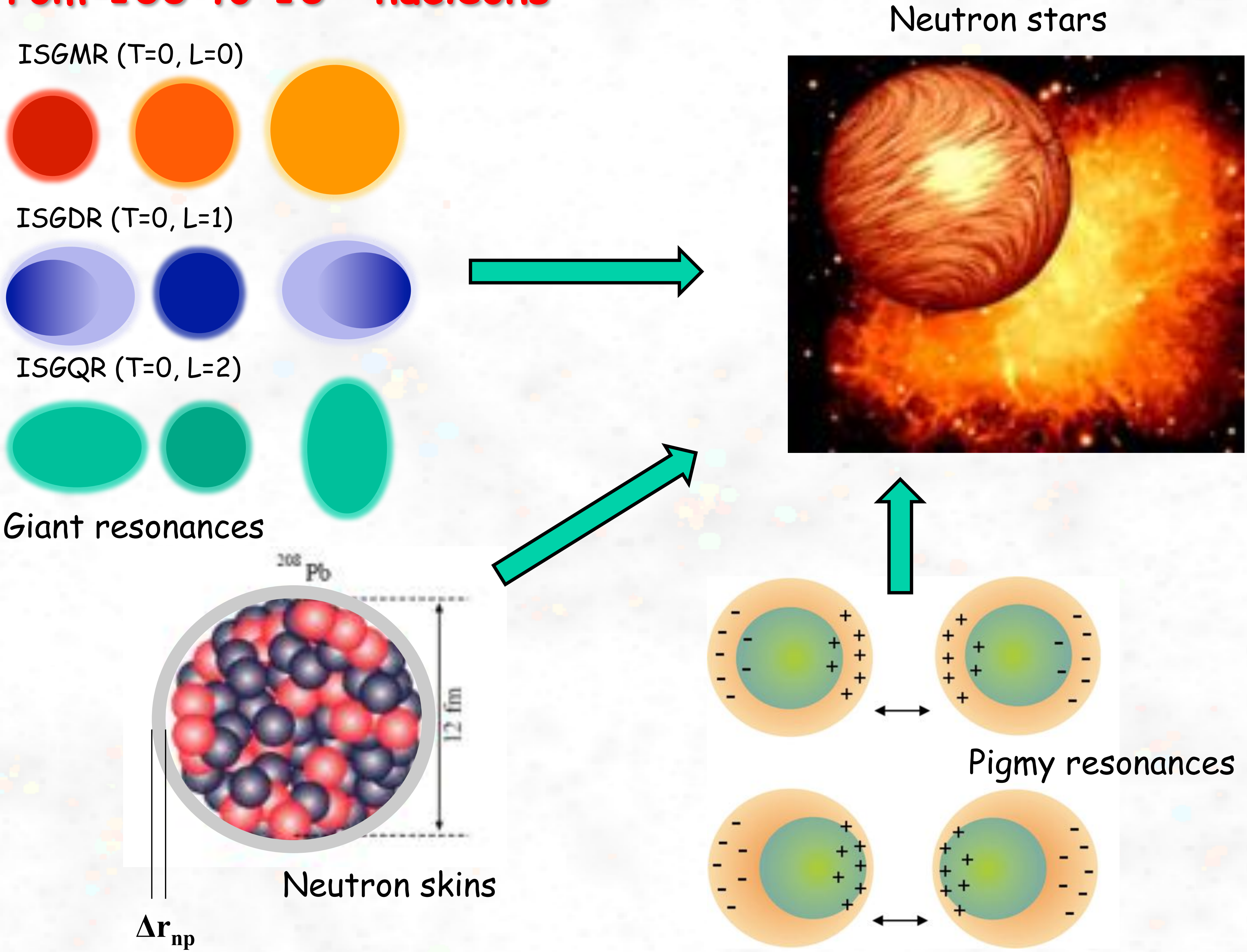

CNN Regions | U.S. Politics | Money | Entertainment | Tech | Sport | Travel | Style | Features | Video International Edition

'Once in a lifetime find': Dinosaur tail discovered trapped in amber

By Katie Hunt, CNN
Updated 1526 GMT (2326 HKT) December 9, 2016

Experiment

Theory

What ?????????

skeptic

From 100 to 10^{57} nucleons

HF + BCS

$$\Delta_i = \frac{1}{2}\sum_j \frac{G_{ij}\Delta_j}{\sqrt{(\varepsilon_j - \lambda)^2 + \Delta_j^2}}$$

HFB

$$\begin{pmatrix} h_{HF} - \lambda & \Delta \\ -\Delta & -h_{HF} + \lambda \end{pmatrix}\begin{pmatrix} u_k \\ v_k \end{pmatrix} = E_k \begin{pmatrix} u_k \\ v_k \end{pmatrix}$$

v_{NN}^{eff} = Skyrme + pairing force

$$V = V_0 \left[1 - \eta\left(\frac{\rho(\mathbf{r})}{\rho_0}\right)^{\alpha}\right]\delta(\mathbf{r}_1 - \mathbf{r}_2), \qquad \rho_0 = 0.16\ \mathrm{fm},$$

$$\eta = \begin{cases} 0, & \text{"volume" pairing} \\ 1, & \text{"surface" pairing} \\ 1/2, & \text{"mixed" pairing} \end{cases}$$

Pairing

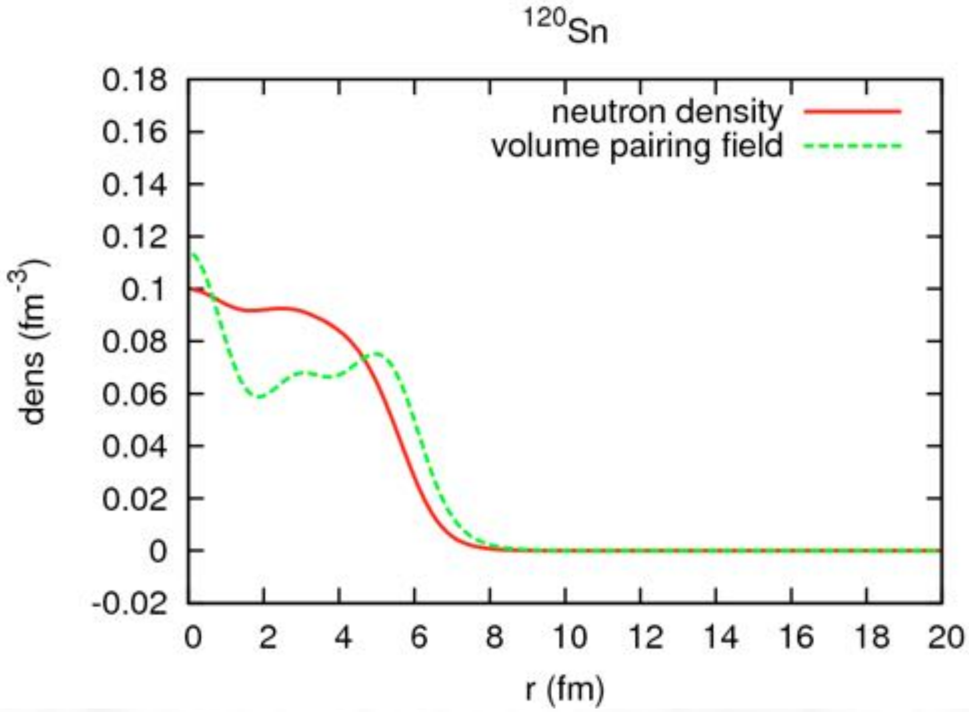

^{120}Sn
neutron density
volume pairing field
dens (fm^{-3})
r (fm)

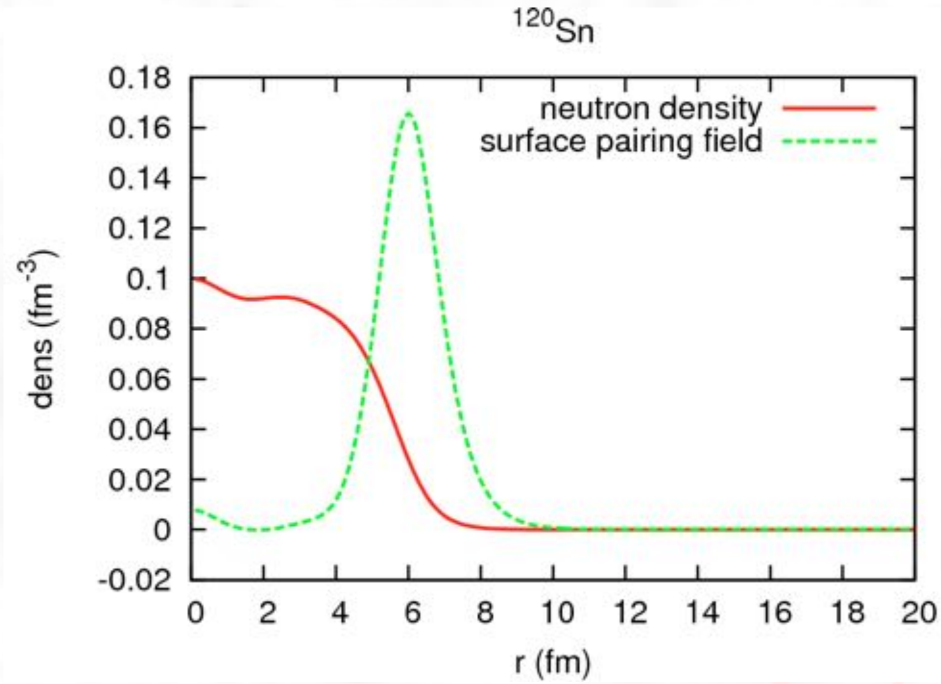

^{120}Sn
neutron density
surface pairing field
dens (fm^{-3})
r (fm)

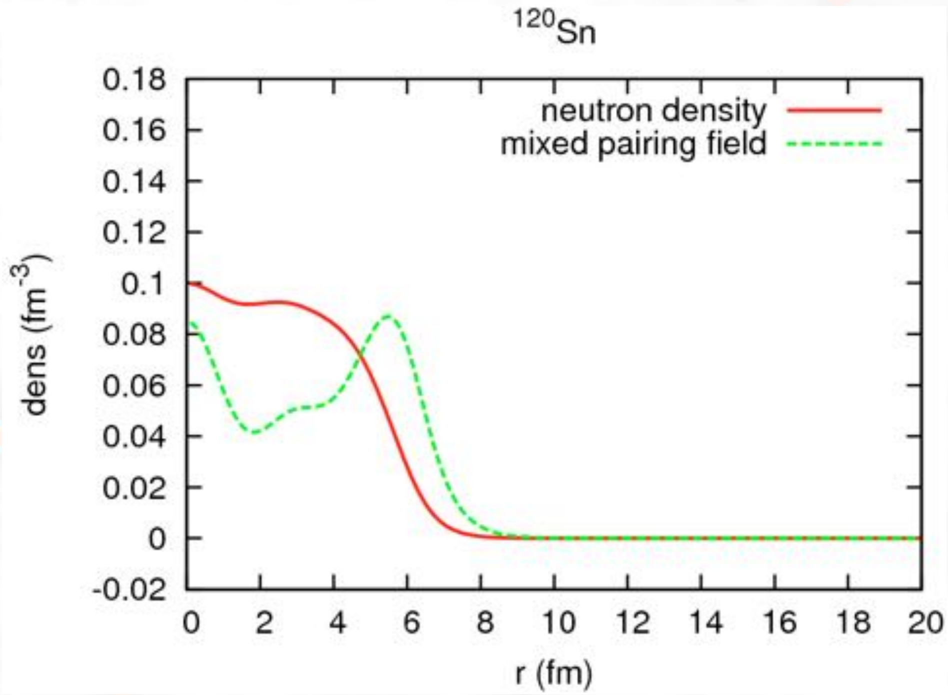

^{120}Sn
neutron density
mixed pairing field
dens (fm^{-3})
r (fm)

Pairing Measure

three-point

$$\Delta^{(3)} = \frac{1}{2}(-1)^N \left[B(N-1) + B(N+1) - 2B(N)\right]$$

four-point

$$\Delta^{(4)} = \frac{1}{4}(-1)^N \left[3B(N-1) - 3B(N) - B(N-2) + B(N+1)\right]$$

or higher

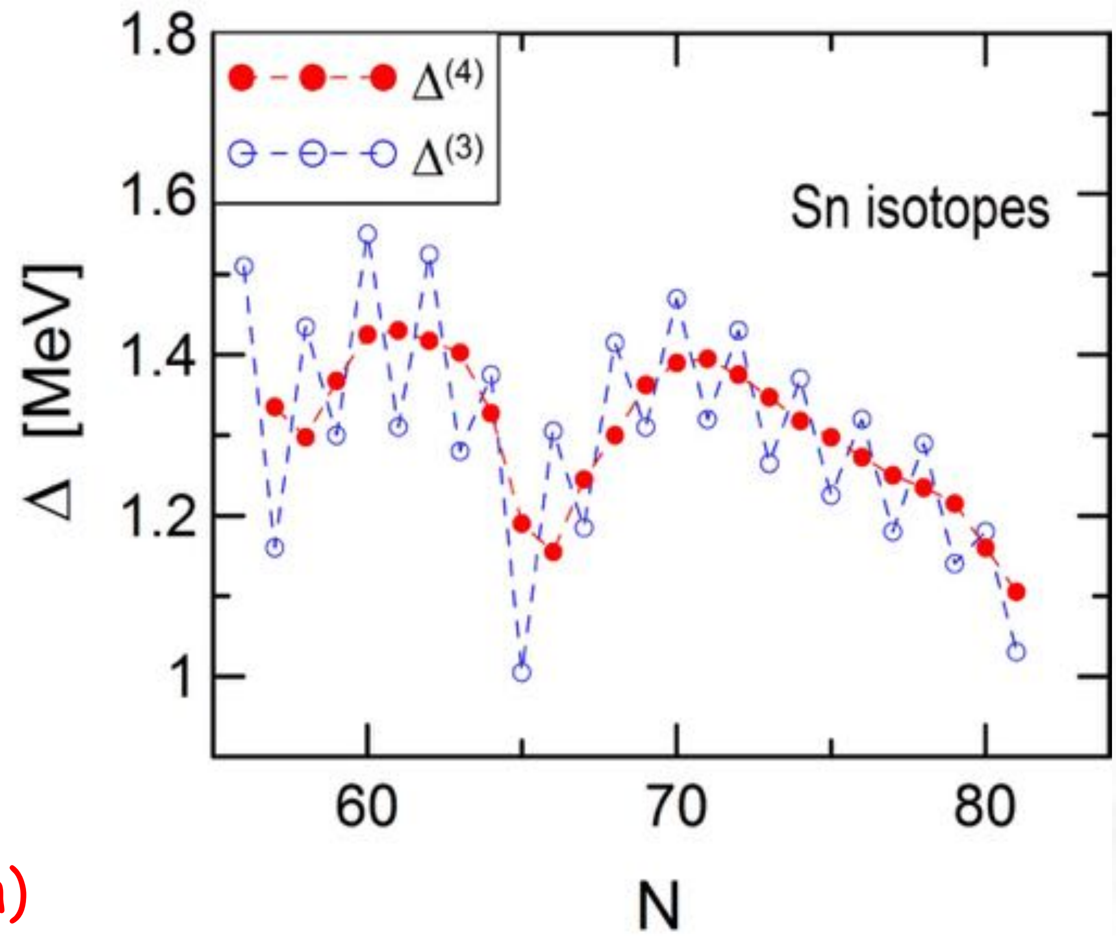

From experiment:

- $\Delta^{(3)}$ larger for $(-1)^N = +1$
- $\Delta^{(3)}$ smaller for $(-1)^N = -1$
- $\Delta^{(4)}$ reflects average of $\Delta^{(3)}$ (N) and $\Delta^{(3)}$ (N-1)

($\Delta^{(4)}$ no additional information)

Pairing vs Binding

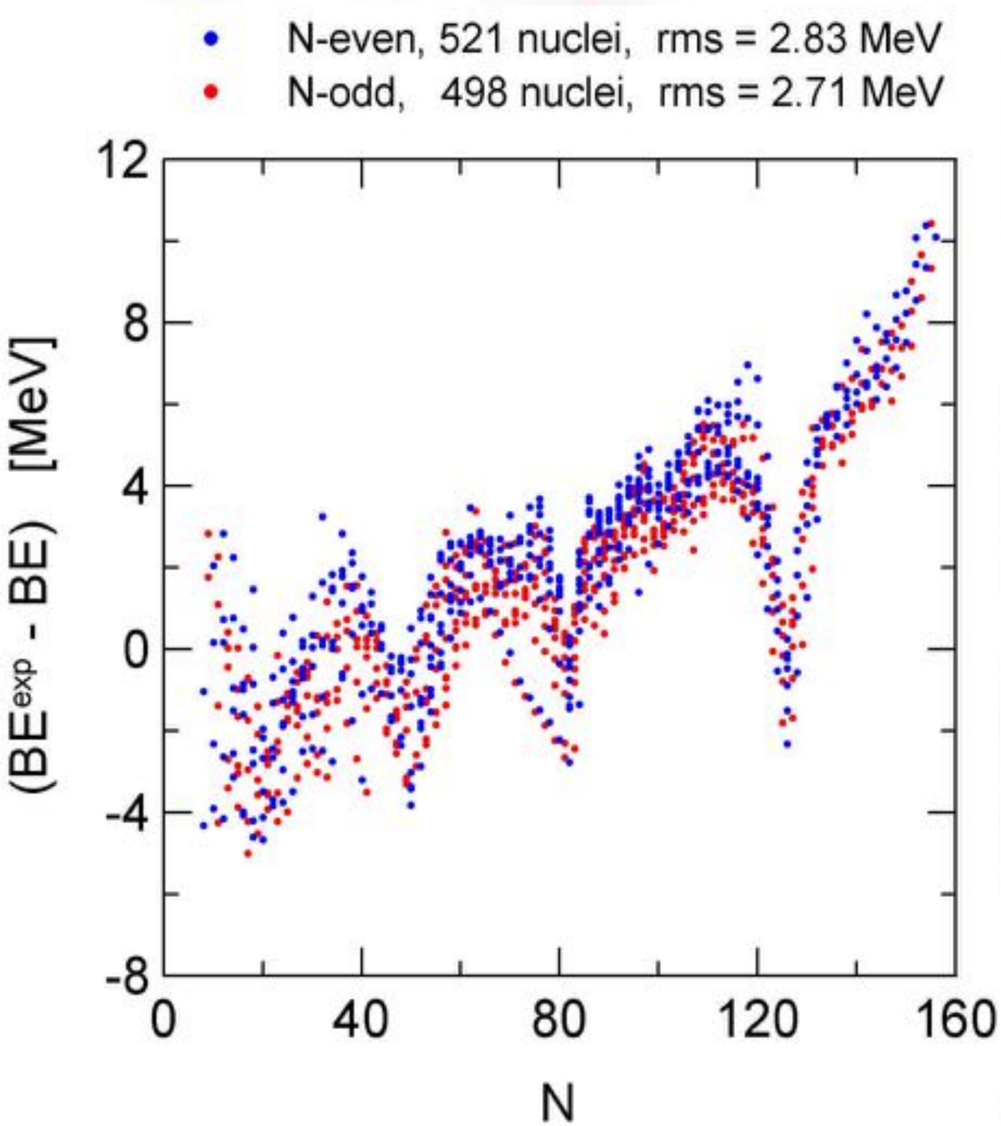

Separation energies staggering

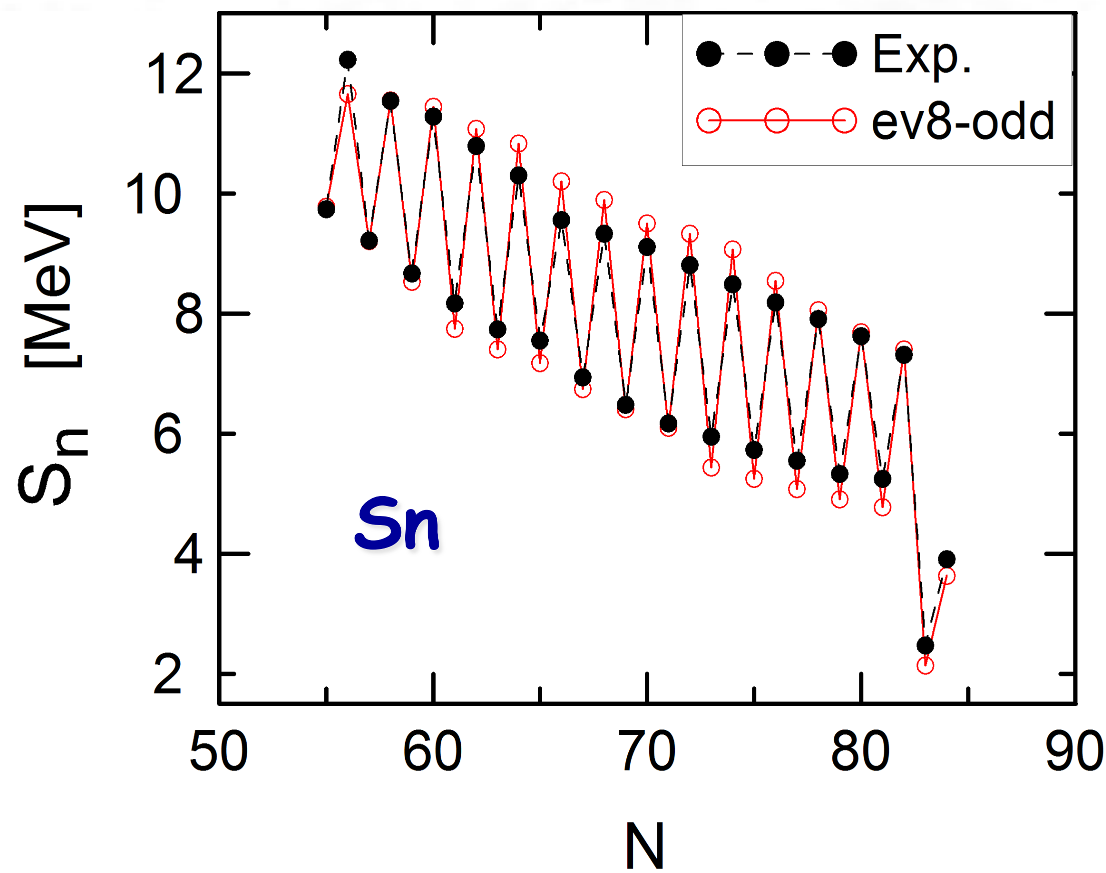

G. Bertsch, CB, for the UNEDF (2007).

Pairing vs Level Properties

$$\Delta^{(3)} = \frac{1}{2}(-1)^N\left[B(N-1)+B(N+1)-2B(N)\right] \;\Rightarrow\; 2(-1)^N\Delta^{(3)} \cong \frac{\partial^2 B}{\partial N^2} = \frac{\partial\lambda}{\partial N} = \frac{1}{g(\lambda)}$$

Fermi energy ($\lambda = \partial B/\partial N$)   s.p. level density ($g(e) = dN/\partial e$)

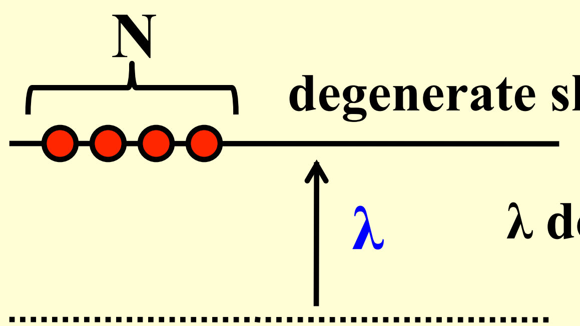

λ does not vary with N → $\Delta^{(3)} = 0$

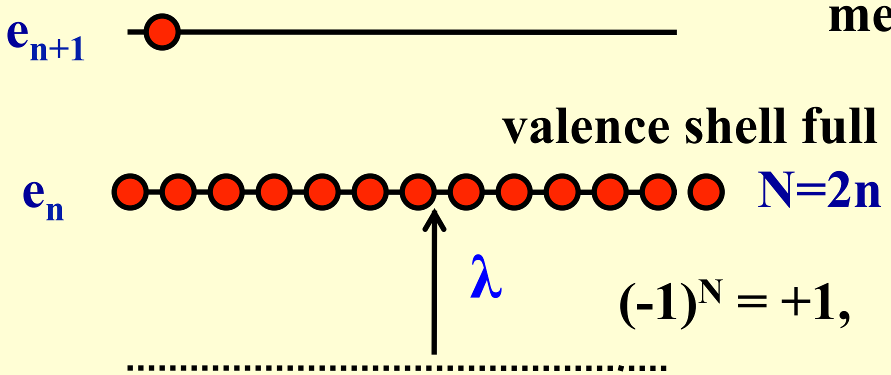

measure of gap in single-particle spectrum

$(-1)^N = +1$, $d\lambda/dN \approx e_{n+1} - e_n$ → $\Delta^{(3)} = (e_{n+1} - e_n)/2$

Jahn-Teller mechanism: spherical symmetry spontaneously broken

⇒ (2j+1) → double-degenerate orbits ⇒ $\Delta^{(3)}$ alternates for $(-1)^N$ = + and -

Pairing vs Level Properties

Macroscopic-microscopic model:

$$B = E_{sp} - \tilde{E}_{sp} + E_{macro}, \qquad E_{sp} = \sum_{k=1}^{A} e_k$$

$$E_{macro} = \cdots + a_I \frac{(N-Z)^2}{A}, \qquad a_I = 23\ \text{MeV}$$

$$\Delta^{(3)} = \frac{23}{A}\ \text{MeV}$$

$$\tilde{E}_{sp}\ \text{contribution}: \quad g(\lambda) = \frac{3a}{\pi^2}, \ a \cong \frac{A}{8}\ \text{MeV}$$

$$\Delta^{(3)} \cong -\frac{1}{g(\lambda)} \cong -\frac{25}{A}\ \text{MeV}$$

$$\Delta^{(3)}(N) \cong -\frac{1}{2}\delta e$$

$$+\ \text{LDM corrections}$$

$$2\left[\Delta^{(3)}(\text{even}) - \Delta^{(3)}(\text{odd})\right] \cong e_{n+1} - e_n$$

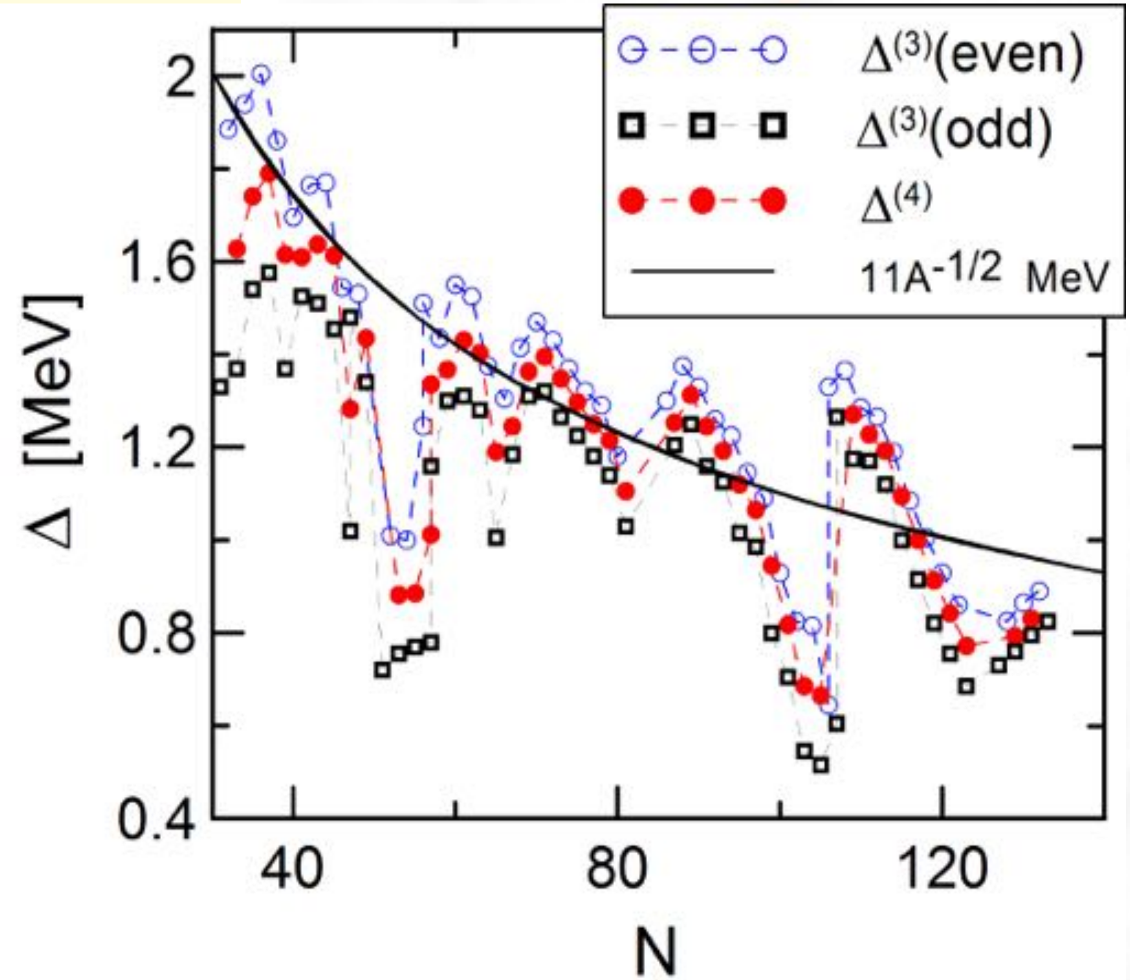

Satula, Dobaczewski, Nazarewicz, PRL 81, 3599 (1998).

Global properties

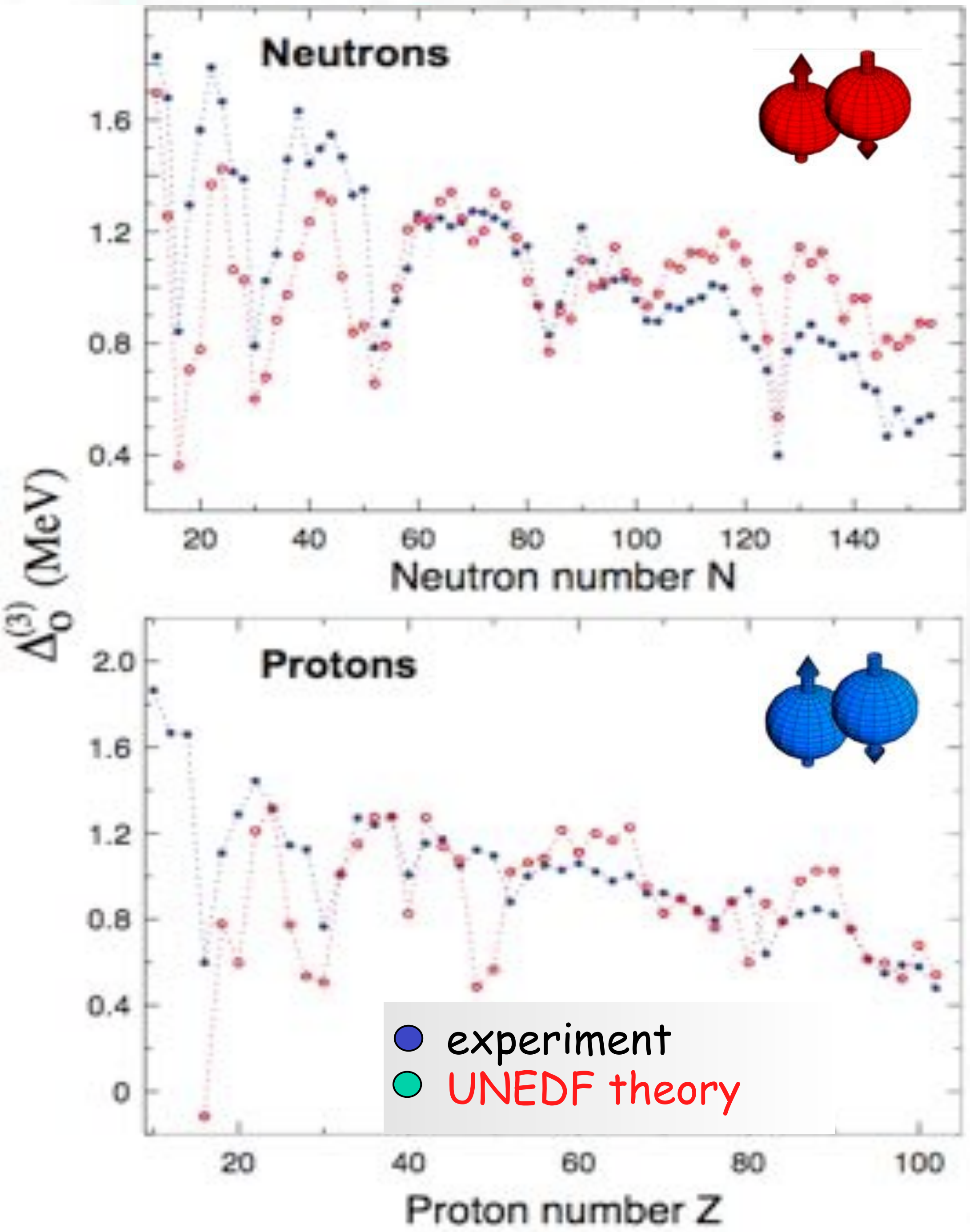

- Mass tables for 2,400 nuclei
- Pairing rms contribution to binding

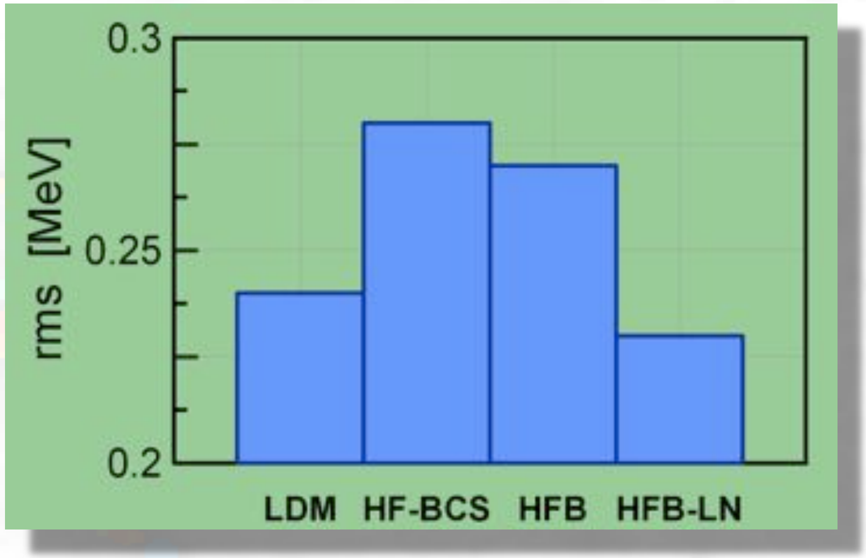

Bertsch, CB, Nazarewicz, Schunck, Stoitsov, PRC 79, 0343306 (2009)

Isovector pairing

CB, Hongfeng Lu, Sagawa,
PRC 80, 027303 (2009)

$$v_{pair}(\mathbf{r},\mathbf{r}') = v_0\left[1-(1-\delta)\eta_s\left(\frac{\rho}{\rho_0}\right)^{\alpha_s} - \delta\eta_n\left(\frac{\rho}{\rho_0}\right)^{\alpha_n}\right]\delta(\mathbf{r},\mathbf{r}')$$

$$\rho = \rho_n + \rho_p$$

$$\delta = \frac{\rho_n - \rho_p}{\rho}$$

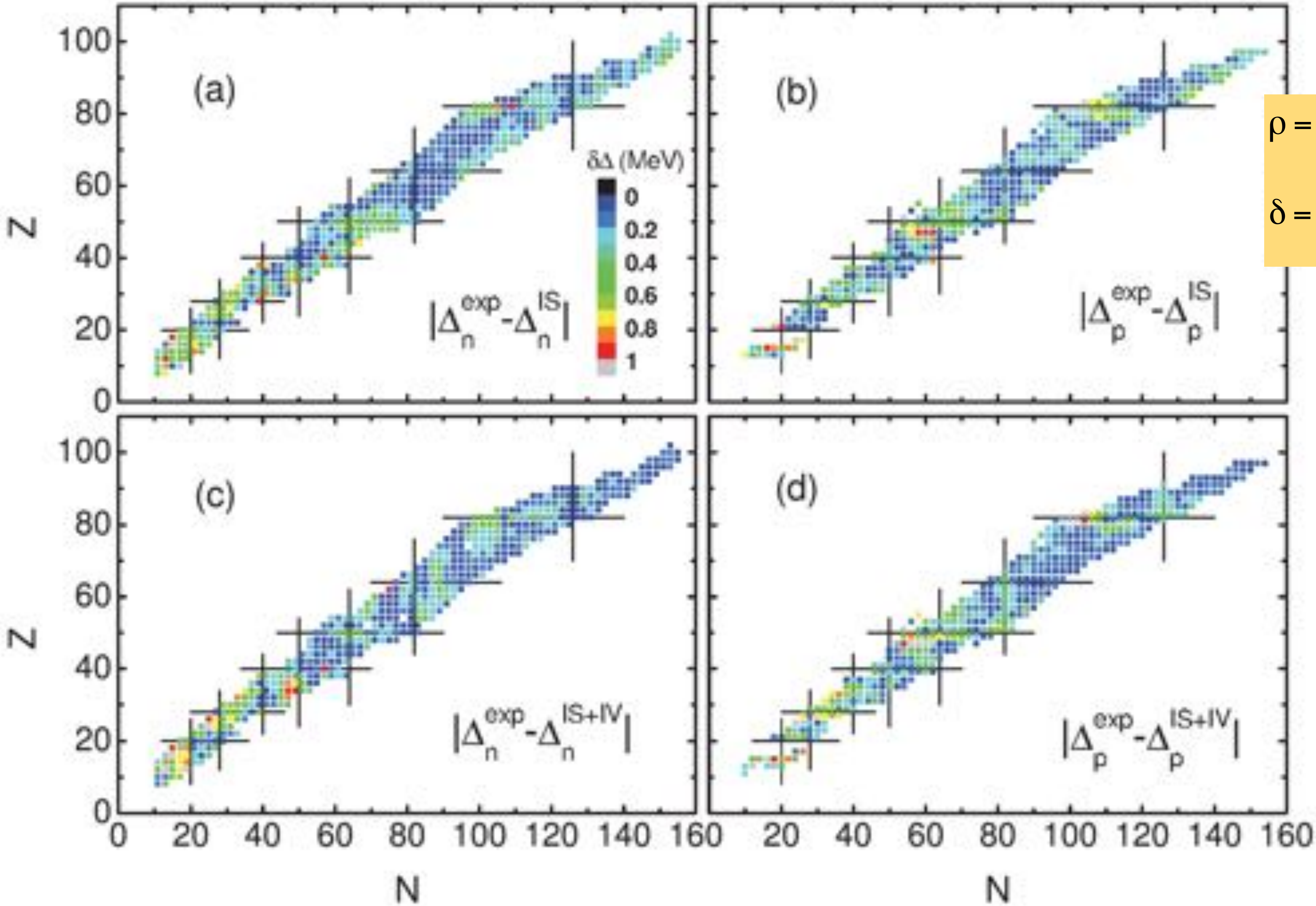

Isovector pairing vs Nuclear Radii

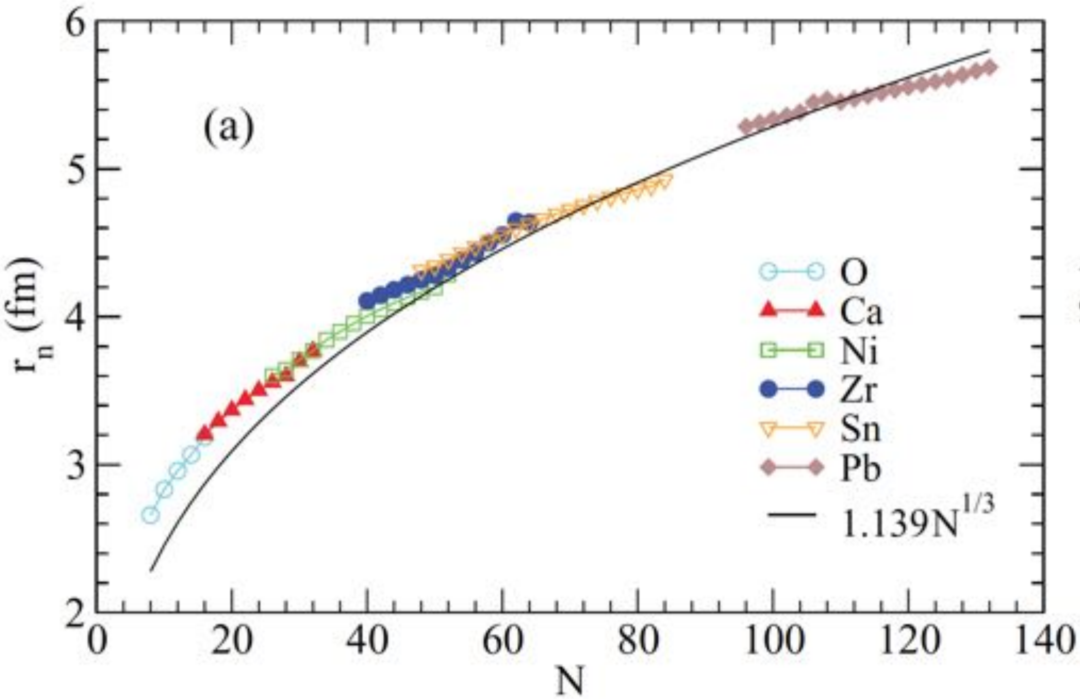

IS + IV pairing

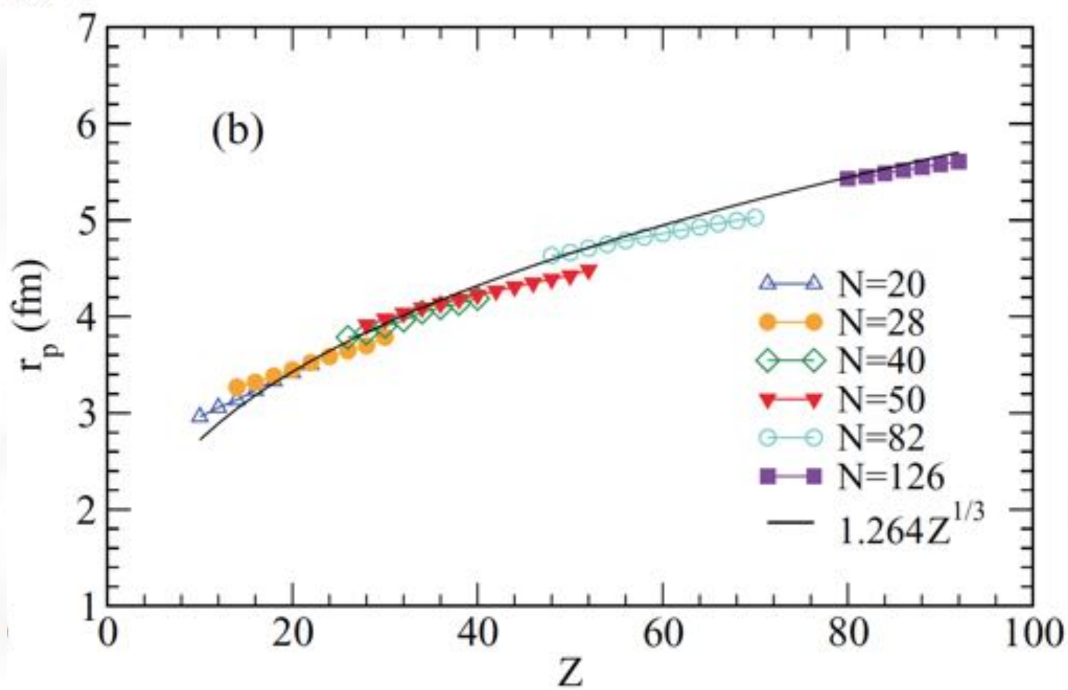

CB, Hongliang Liu, Sagawa,
PRC 85, 014321 (2012)

Isovector pairing & Nuclear Skins

IS+IV pairing

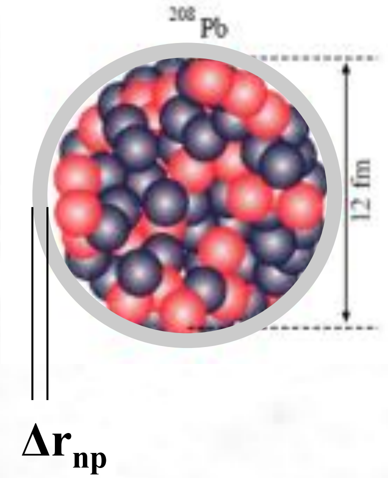

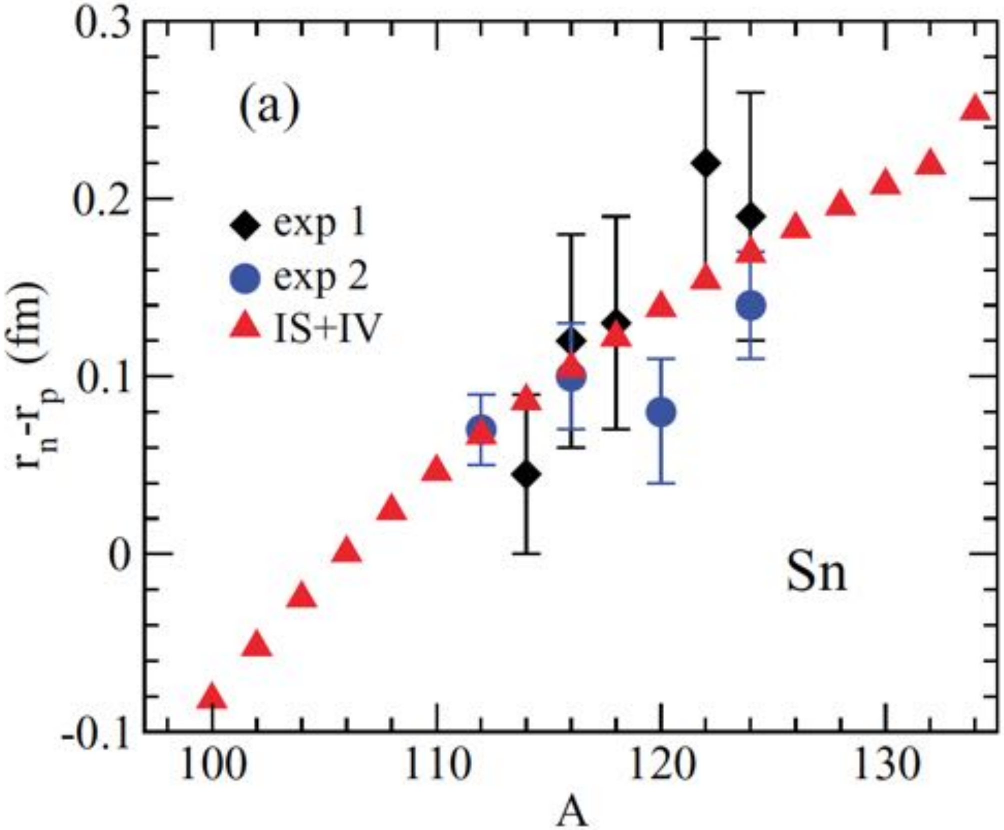

CB, Hongliang Liu, Sagawa,
PRC 85, 014321 (2012)

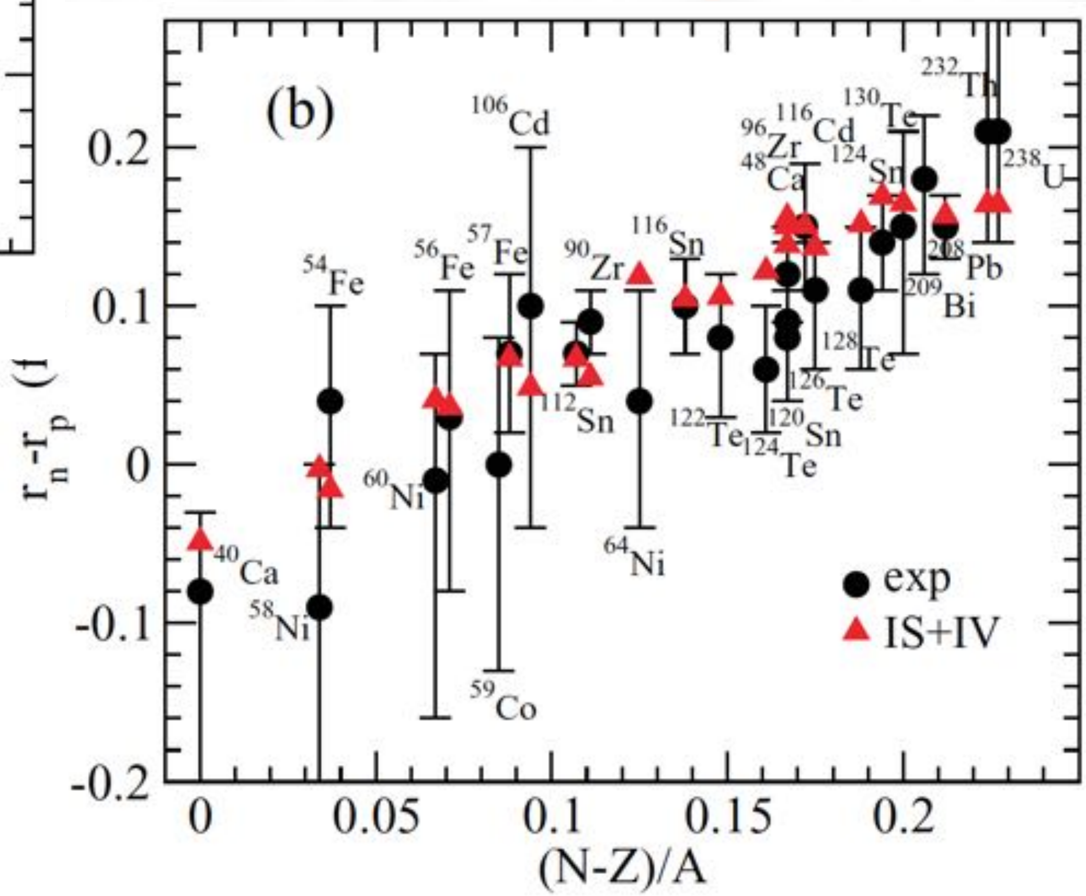

Radii from spin-dipole resonances
Krasznahorkay et al., PRL 82, 3216 (1999)

&

Antiprotonic atoms
Trzcinskaet al., PRL 87, 082501 (2001)

QRPA: The Role of Pairing Rearrangement Term

Avogadro, CB, PRC 88, 044319 (2013)

$$h = \frac{\delta E_{kin}}{\delta \rho} + \frac{\delta E_{skyrme}}{\delta \rho} + \frac{\delta E_{pair}}{\delta \rho} + \frac{\delta E_{Coul}}{\delta \rho}$$

- Fully self consistent EWSR = 99.2%
- Without rearrangement in EWSR =116%

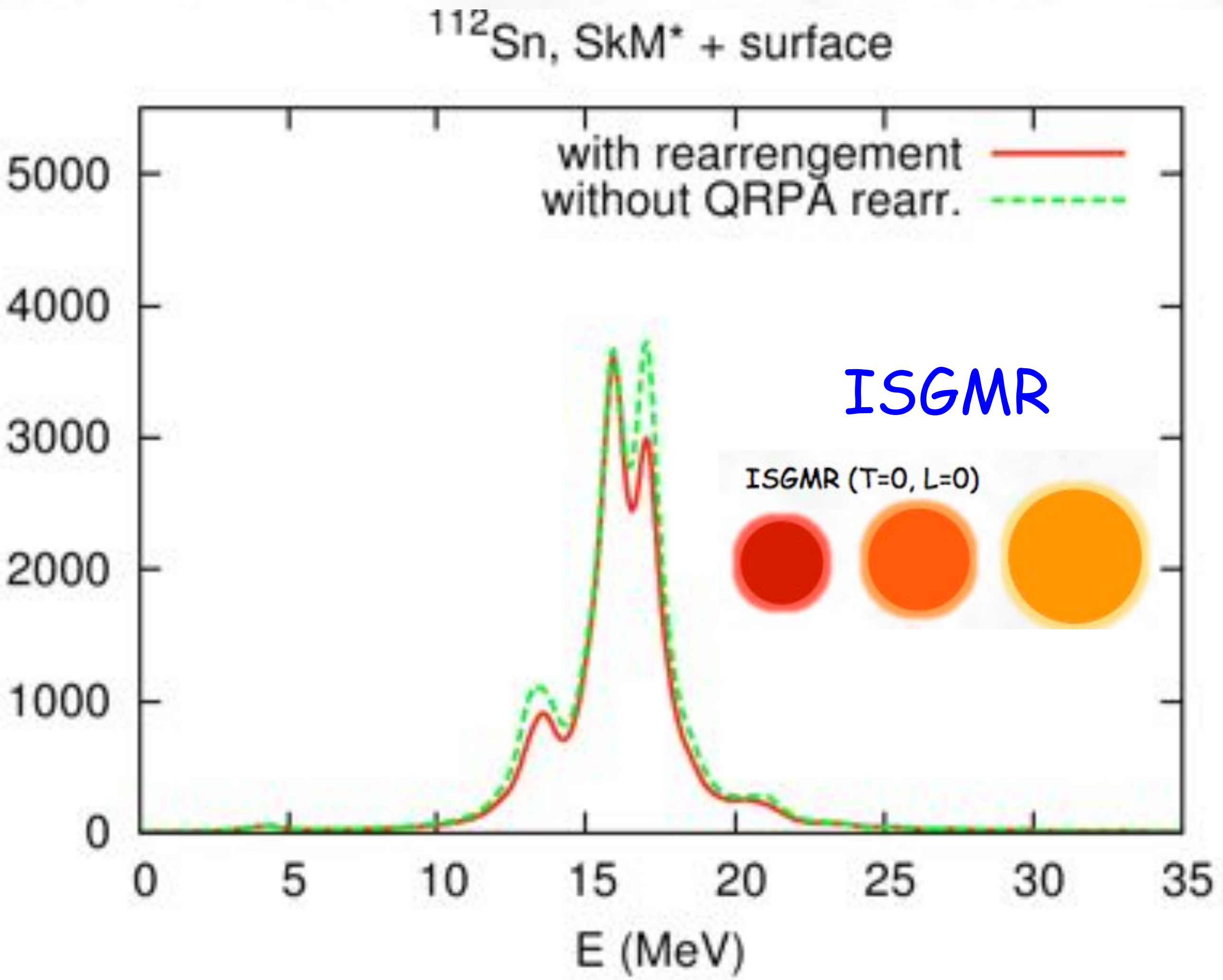

$$\frac{\delta h_{rearr}}{\delta \rho} = \frac{\delta}{\delta \rho}\left(\frac{\delta E_{pair}}{\delta \rho}\right)$$

$\neq 0$ if E_{pair} depends on density

Calculations without rearrangements tend to return higher centroids respect to the fully self-consistent case.

Dependence on Functional

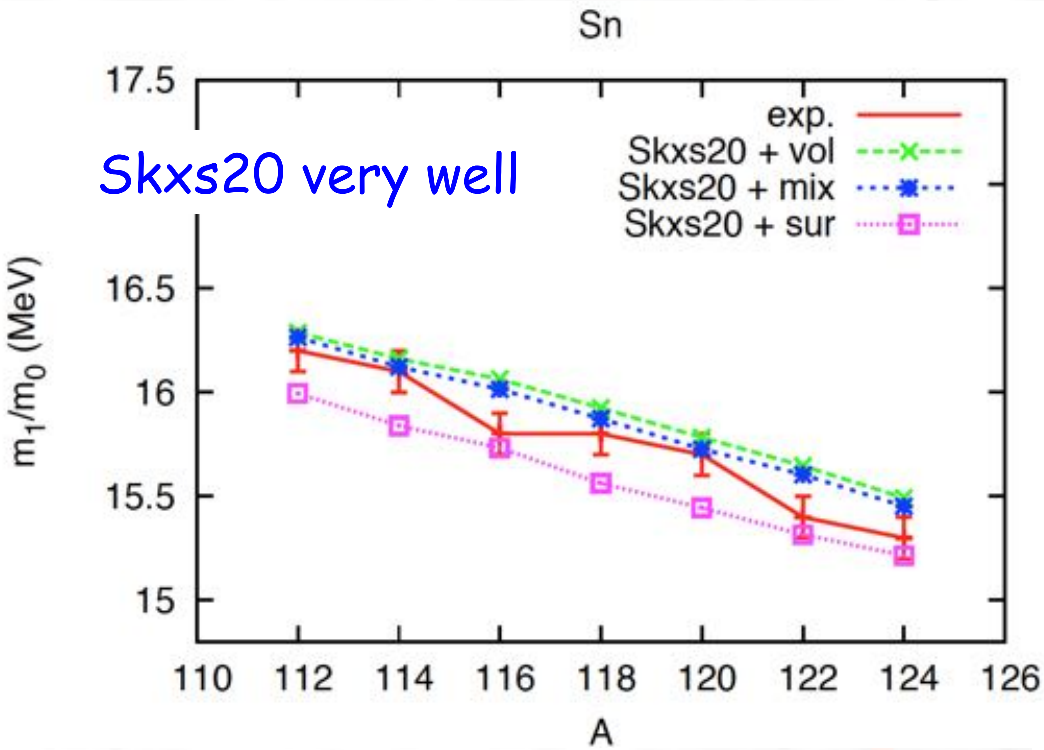

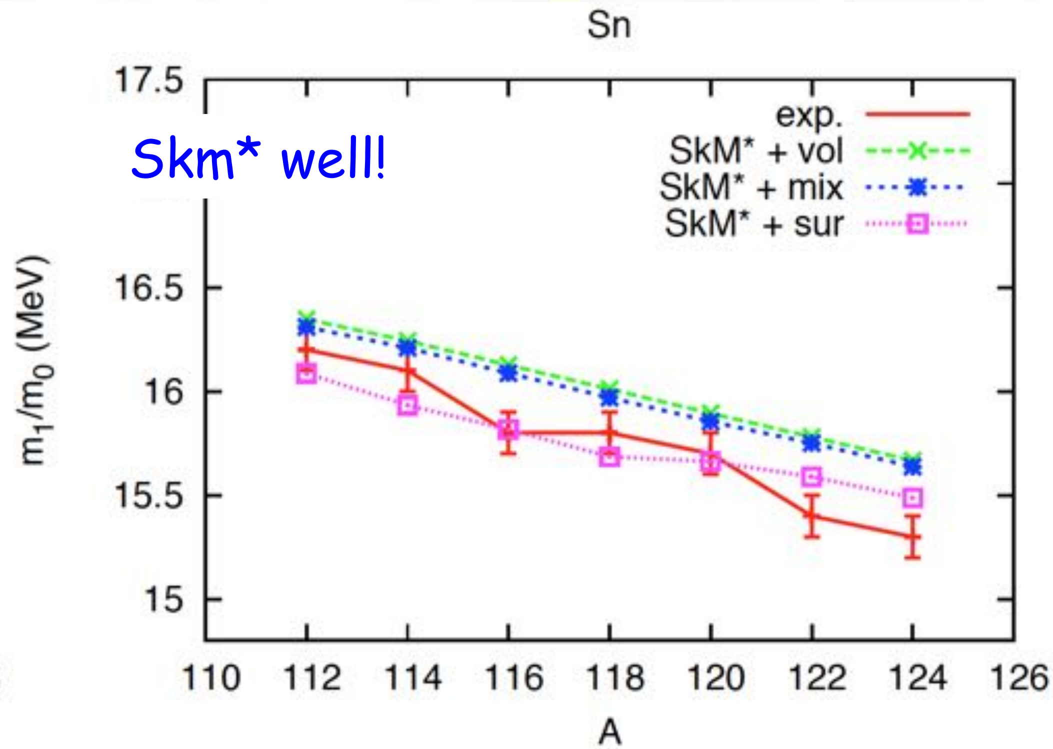

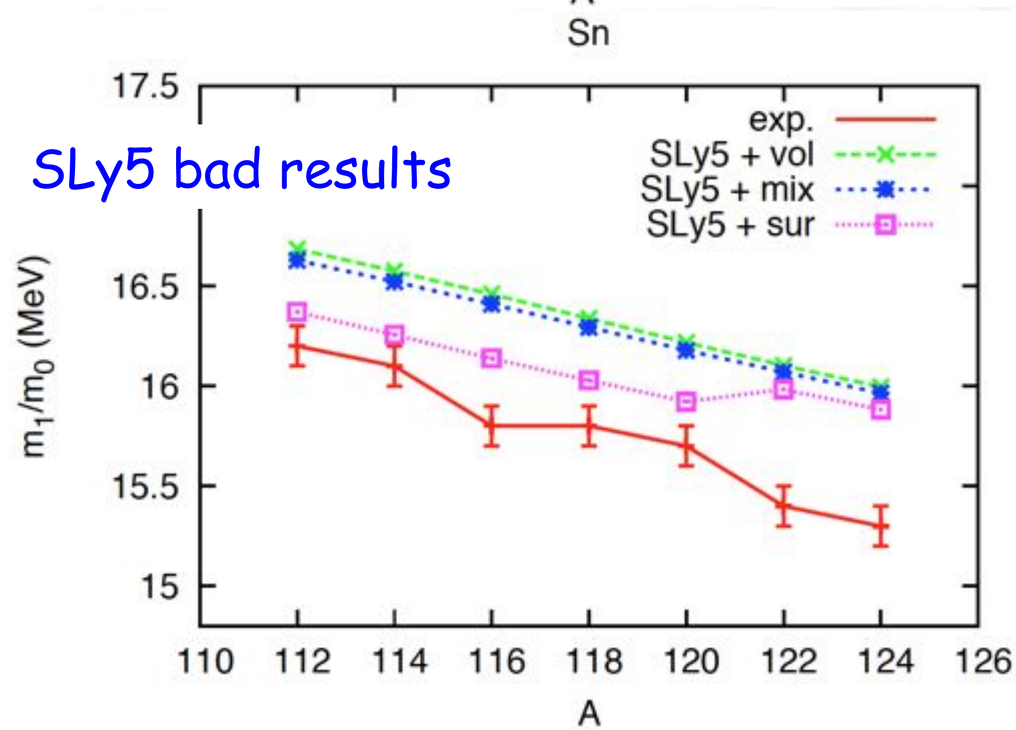

$$S(E) = \sum_j \left| \langle 0 | F_0 | j \rangle \right|^2 \delta\left(E - E_0\right)$$

$$F_0 = \sum_{i=1}^{A} r_i^2$$

$$m_k = \int_0^{\infty} E^k \, S(E) \, dE$$

Isovector pairing

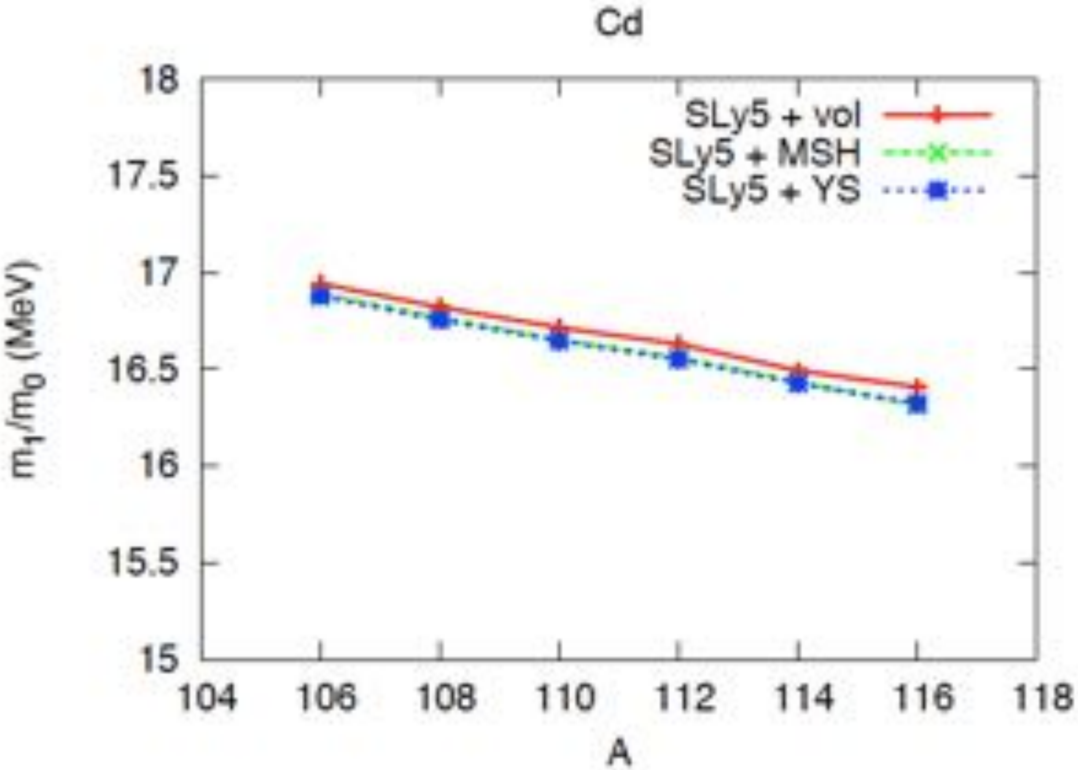

Weakly Improves Centroids of ISGMR

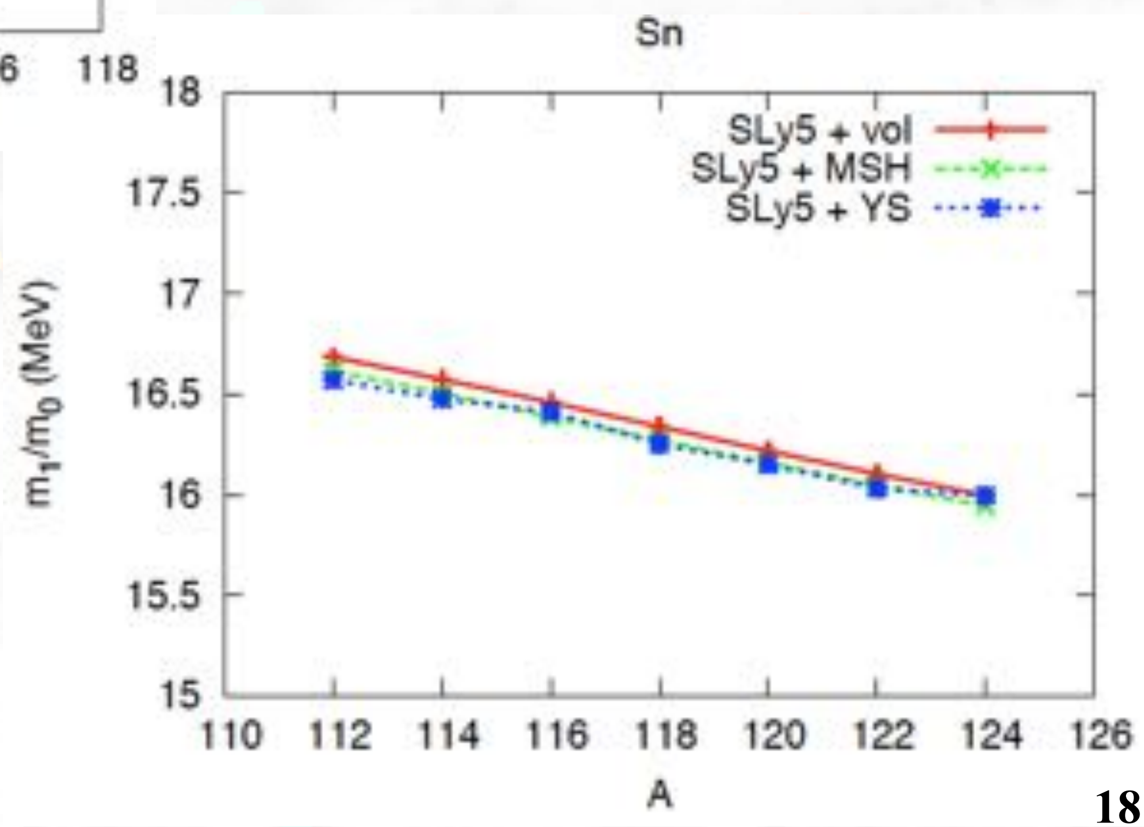

Pairing – ISGMR – Comparison to data

	nucleus	ph	pp	diff.
TAMU/ RCNP	$^{204-206-208}$Pb	SLy5	all	< 0.1
TAMU/ RCNP	^{144}Sm	SkM*	*volume*	- 0.1
TAMU/ RCNP	^{90}Zr	SLy5	all	+ 0.2
	^{92}Zr	SLy5	*volume*	- 0.4
TAMU	^{94}Zr	Skxs20	*surface*	+ 0.8
TAMU	^{92}Mo	SLy5	*volume*	- 1.6
	^{94}Mo	Skxs20	*surface*	+ 0.0
RCNP	$^{112-114-118-120}$Sn [4]	Skxs20	*mixed*	< 0.1
	$^{122-124}$Sn [4]	Skxs20	*surface*	< 0.1
	^{116}Sn [4]	SkM*	*surface*	< 0.1
TAMU	$^{112-124}$Sn [35]	Skxs20	*surface*	≈ 0.8
	^{116}Sn [35]	Skxs20	*surface*	+ 0.2
RCNP	$^{106-110-112-114-116}$Cd [6]	Skxs20	*surface*	< 0.1
TAMU	$^{110-116}$Cd [46]	Skxs20	*surface*	≈ 0.9

Avogadro, CB,
PRC 88, 044319 (2013)

ISGMR is better reproduced with the soft interaction Skxs20 ($K_\infty \approx 202$ MeV), in contrast with the generally accepted value for $K_\infty \approx 230$ MeV.

Mean-Field Dynamics

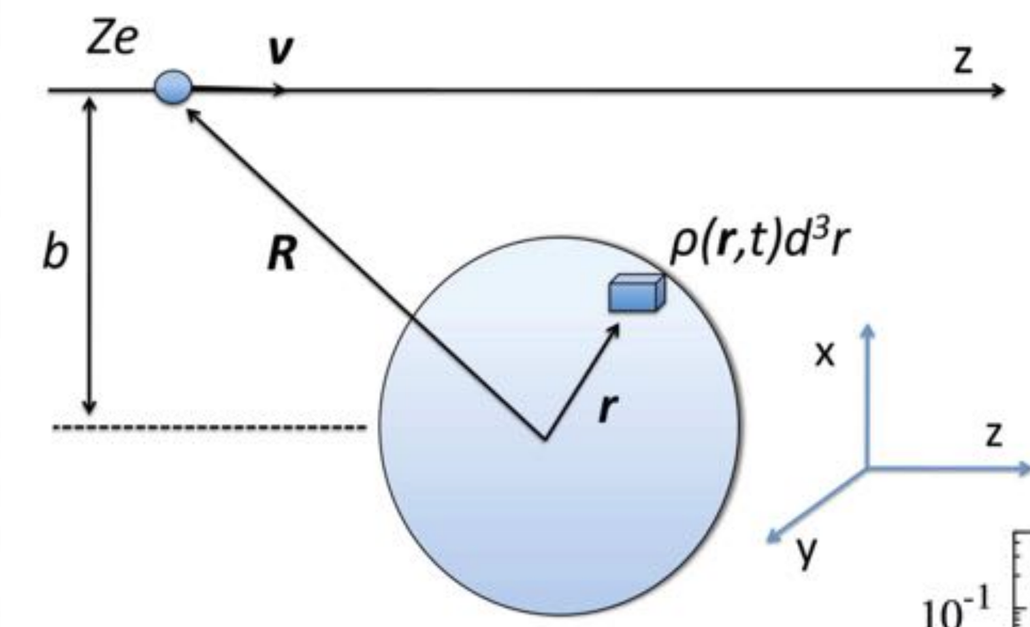

Time dependent superfluid local density approximation (TDSLDA)

Stetcu, CB, Bulgac, Magierski, Roche
PRL 114, 012701 (2015).

Emitted EM radiation

$^{238}U + ^{238}U$ (1 GeV/nucleon)

Skyrme SLy4

Curves are contributions from different orientations

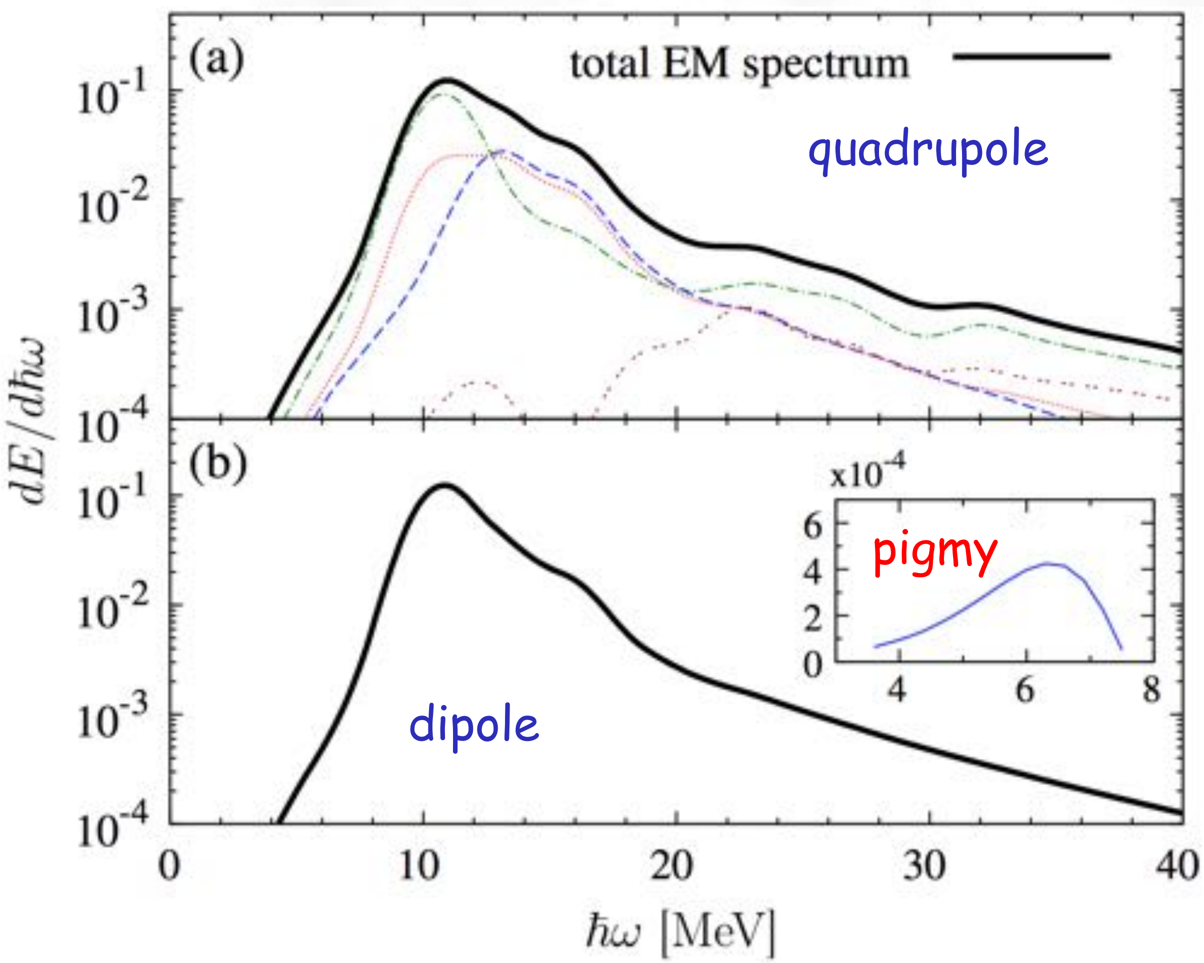

Mean-Field Dynamics

Stetcu, CB, Bulgac, Magierski, Roche
PRL 114, 012701 (2015).

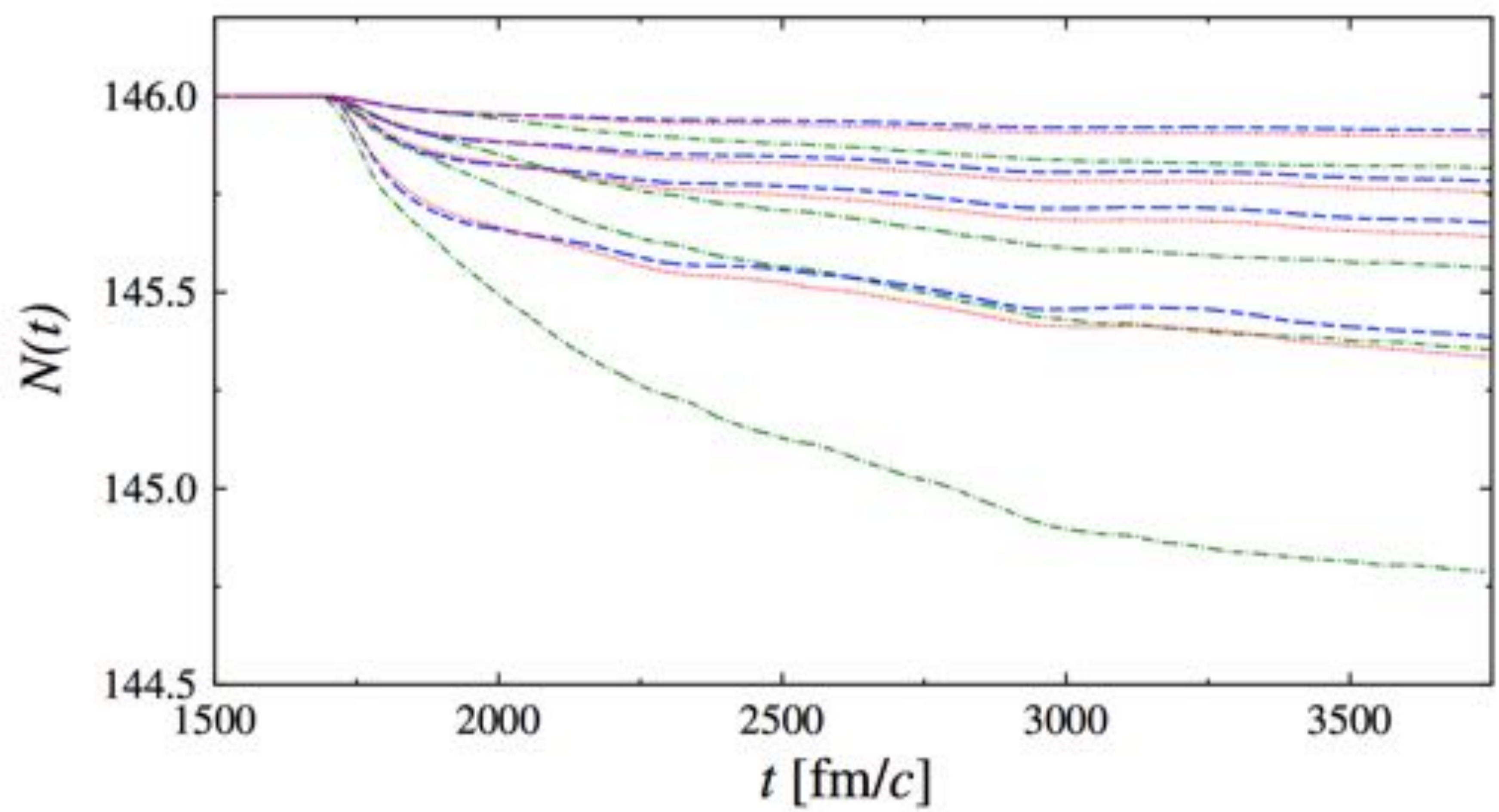

Number of neutrons within 15 fm radius for different impact parameters (12 – 20 fm)

^{238}U + ^{238}U (1 GeV/nucleon)

EM response in neutron-rich nuclei

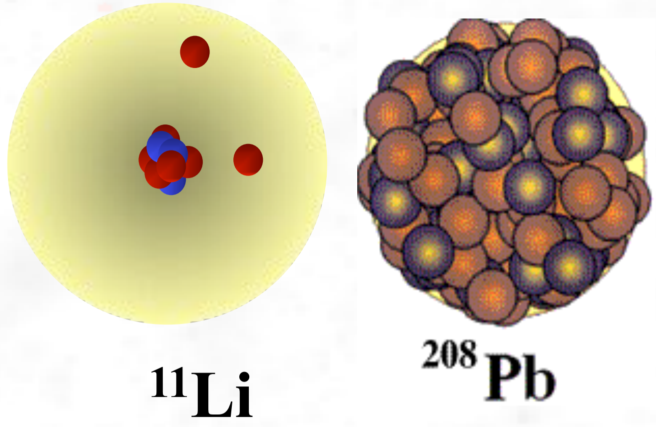

Two-body Cluster: CB, Baur, NPA 480, 615 (1988)
CB, Sustich, PRC 46 , 2340 (1993)

$$\frac{dB(EL)}{dE} \sim \frac{\left(E_x - S_n\right)^{L+1/2}}{E_x^{2L+2}}$$

$$E_r^{(E\lambda)peak} \cong \frac{\lambda + 1/2}{\lambda + 3/2} S_n$$

Cluster RPA: Teruya, CB, Krewald, Dias. Hussein, PRC 43, 2049 (1991)

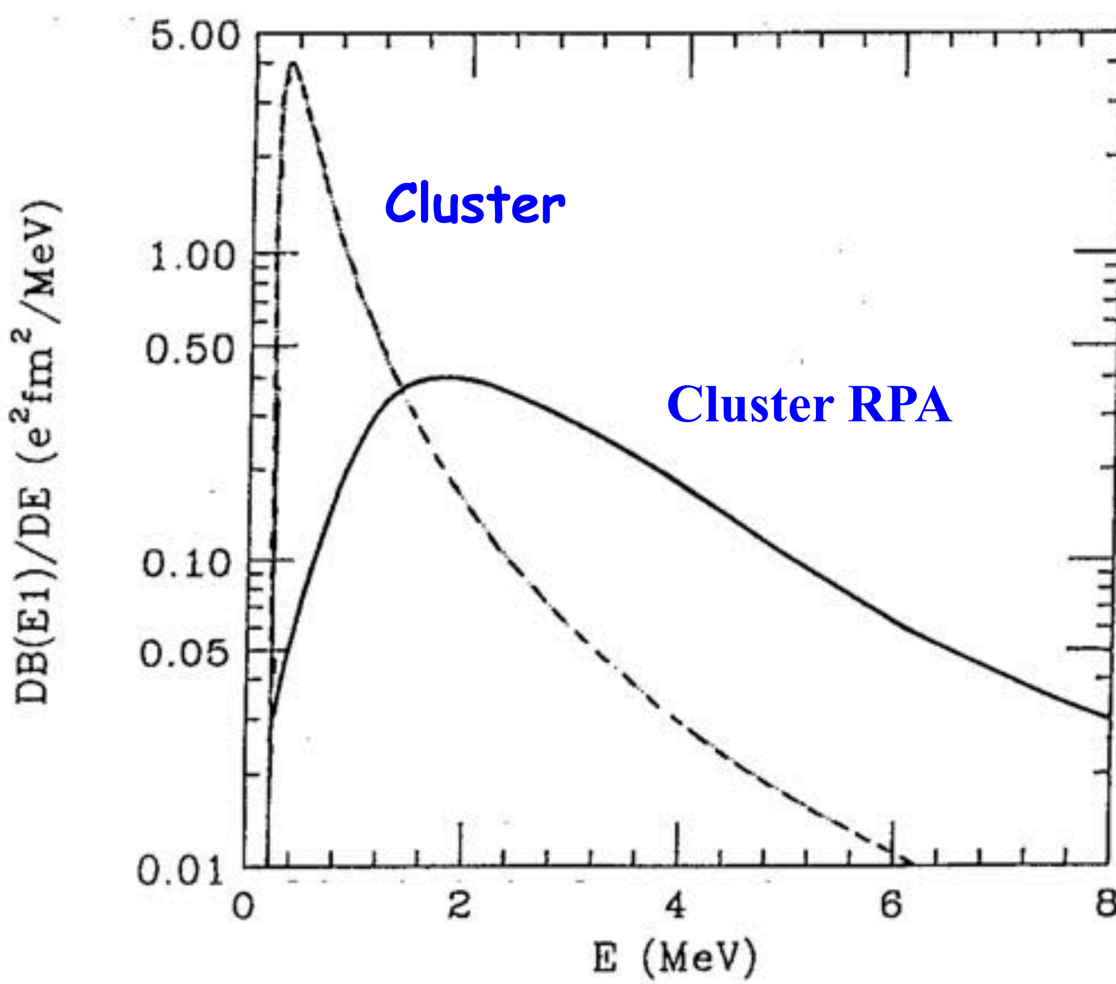

Three-body cluster

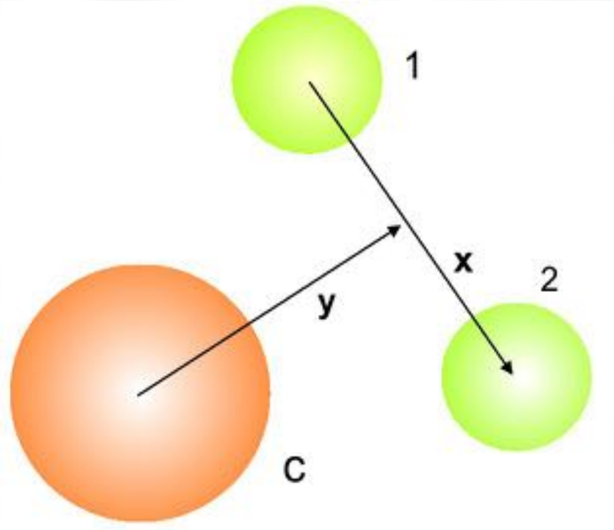

CB, PRC 75, 024606 (2007)

$$\frac{dB(E1)}{dE_r} \propto \frac{E_r^3}{\left(S_{2n}^{\text{eff}} + E_r\right)^{11/2}} \left(1 + FSI\right)^2$$

$$S_{2n}^{\text{eff}} \cong 1.8\, S_{2n}$$

Three-body model

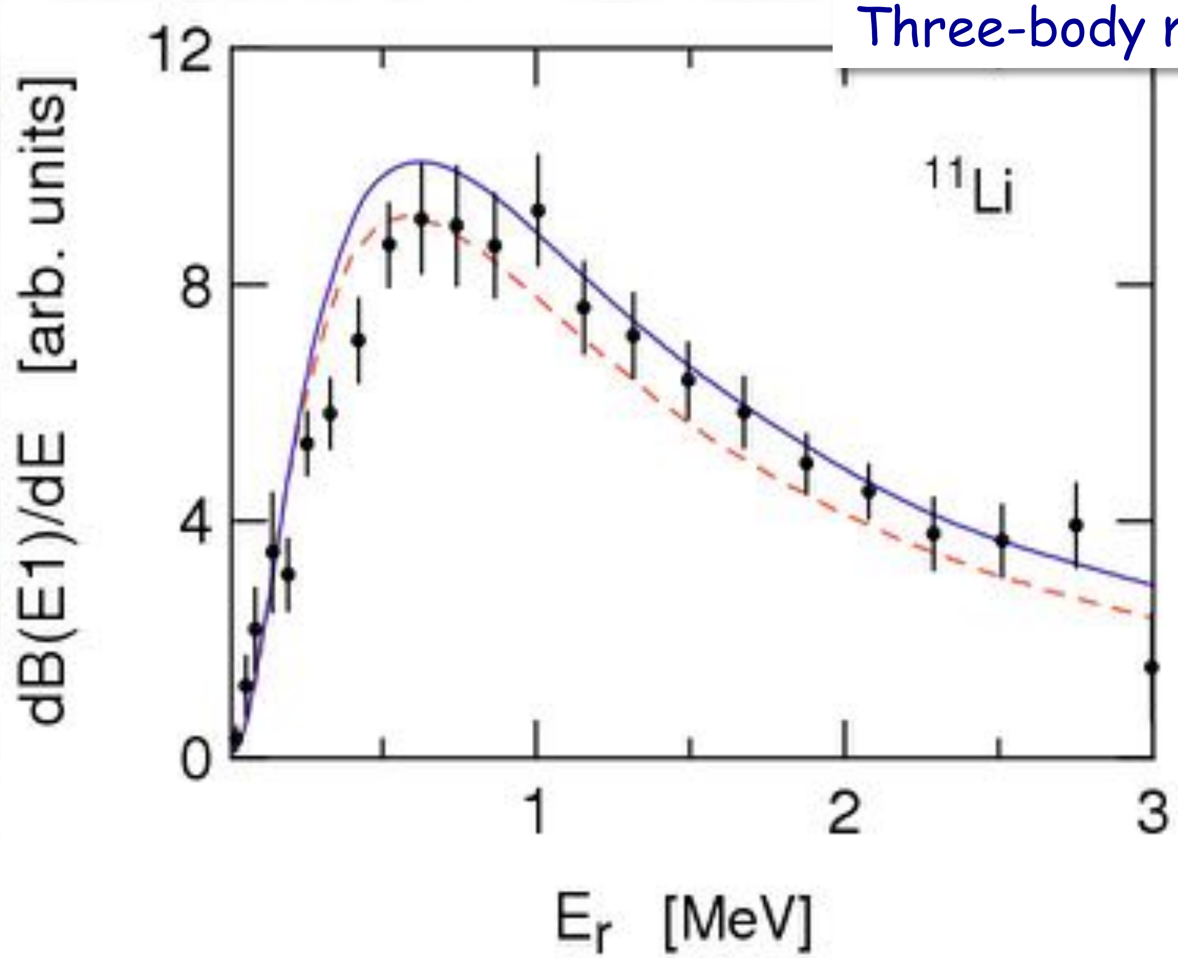

Continuum RPA: CB, Sustich, PRC 46 , 2340 (1993)

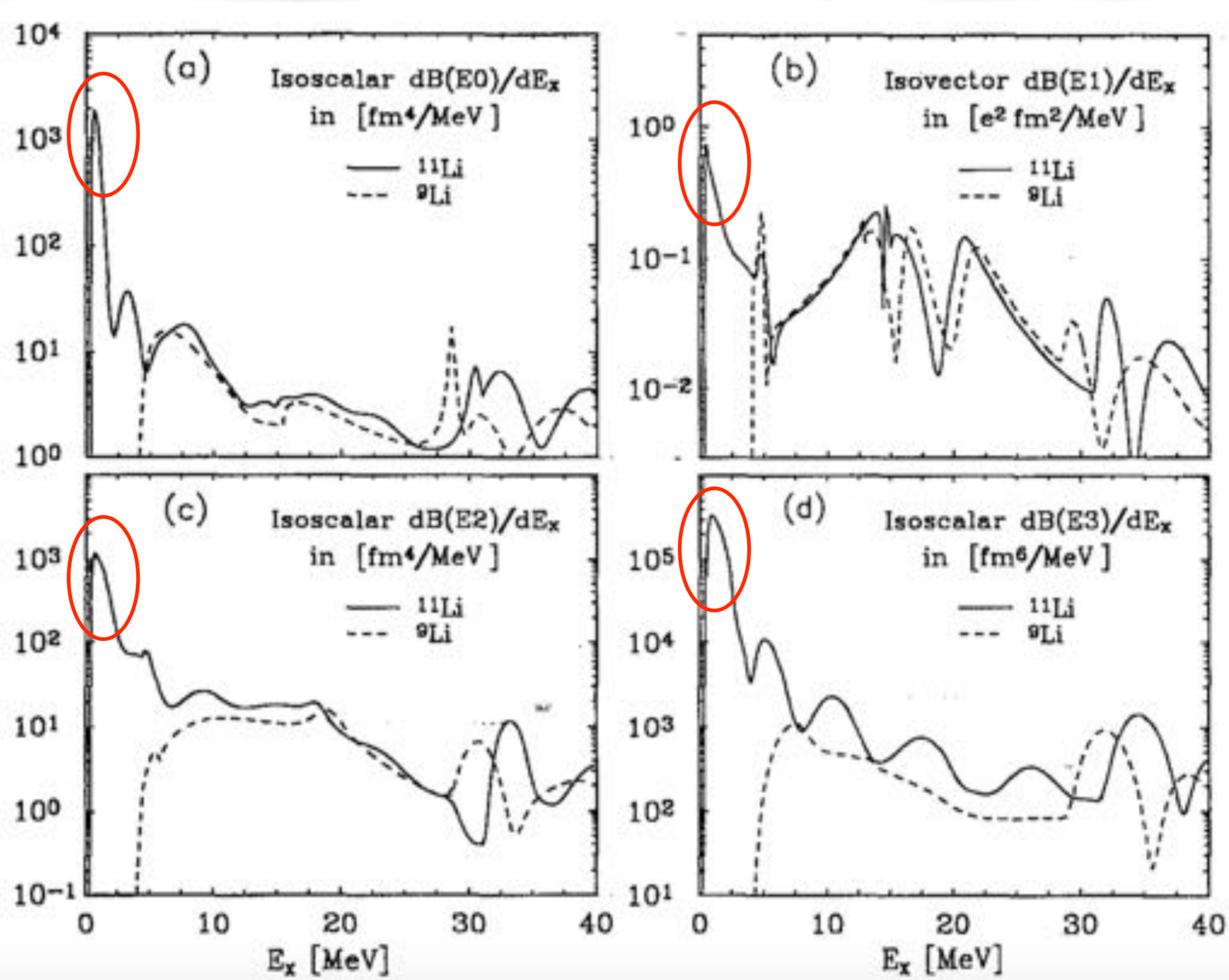

Coulomb excitation of Pigmy Resonances

Rossi et al.
PRL 111 (2013) 242503

Wieland et al.
PRL 102, 092502 (2009)

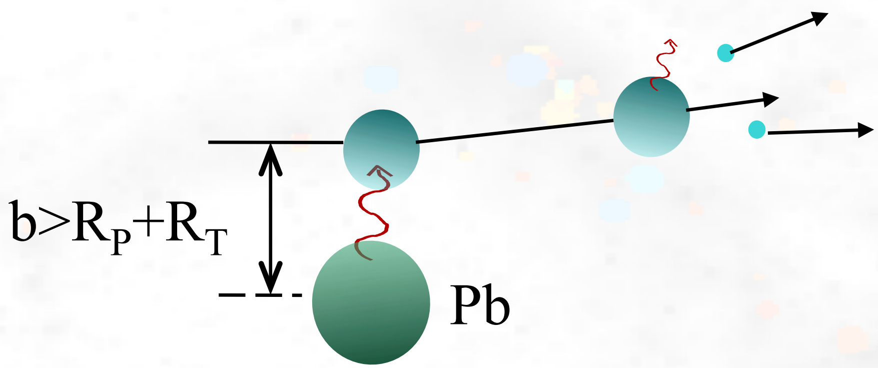

Dipole polarizability

$$\alpha_D = \frac{\hbar c}{2\pi^2}\int_0^\infty \frac{\sigma_\gamma(E)}{E^2}dE$$

$$= \frac{8\pi}{9}\int \frac{dB(E1,E)}{dE}dE$$

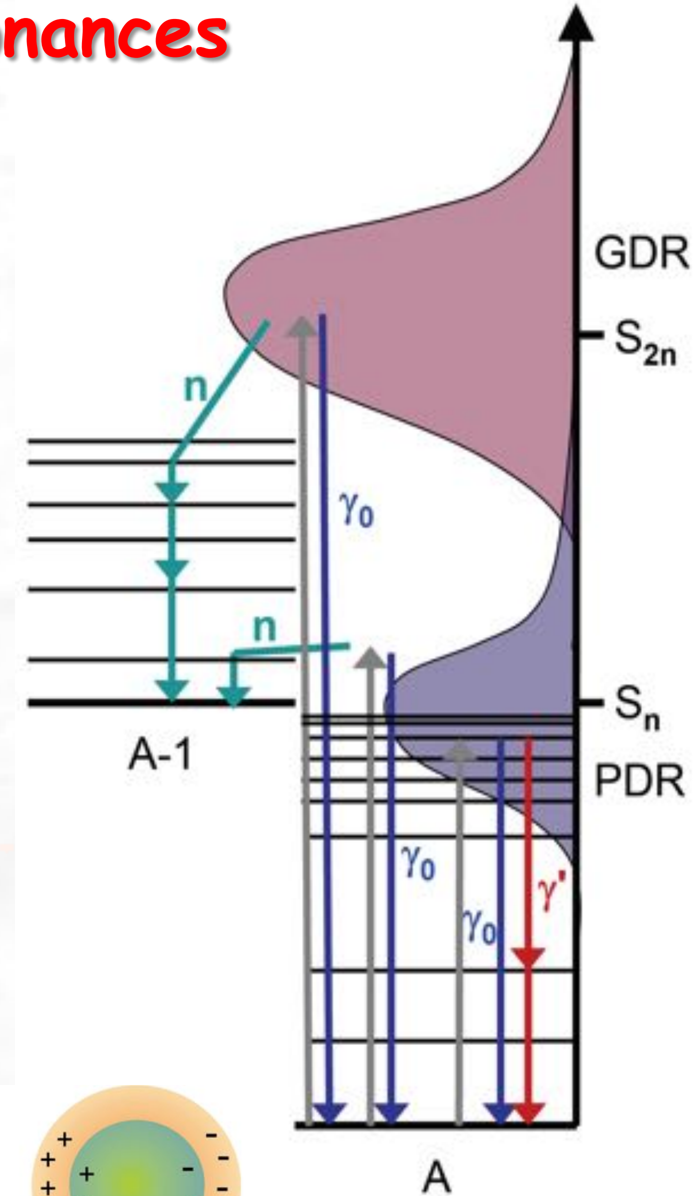

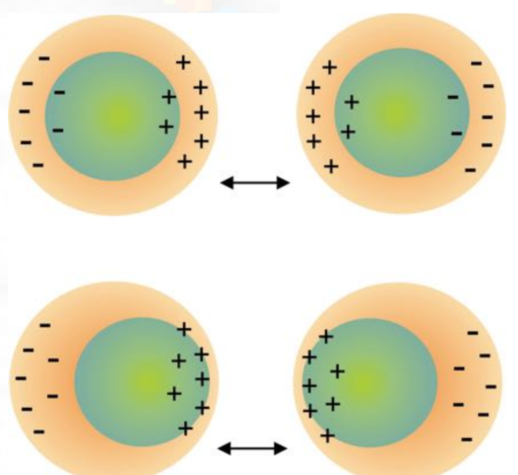

E & M response in heavy neutron-rich nuclei

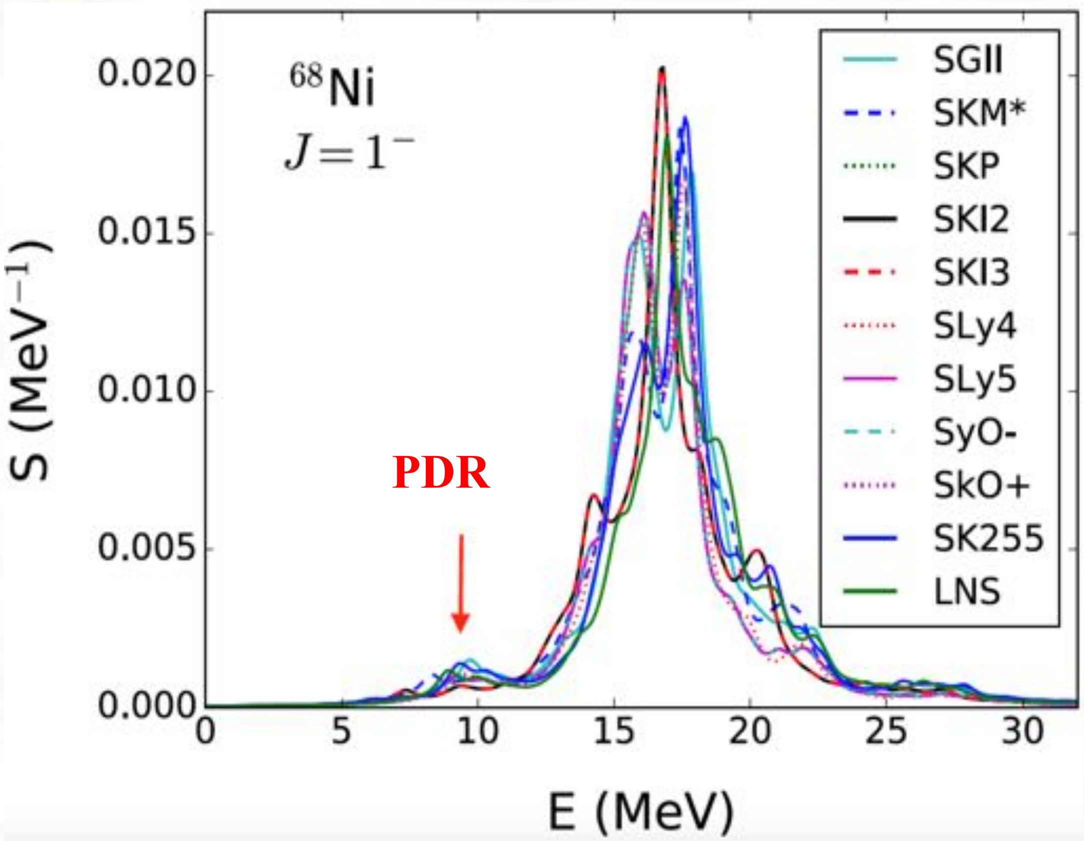

$$S(E) = \sum_{\nu} \left| \left\langle \nu \left\| j_L\left(\frac{Er}{\hbar c}\right) \right\| 0 \right\rangle \right|^2 \delta(E - E_\nu)$$

Colo, Cao, Giai, Capelli,
Comput. Phys. Comm. 184, 142 (2013)

$$\alpha_D = \frac{\hbar c}{2\pi^2} \int_0^\infty \frac{\sigma_\gamma(E)}{E^2} dE$$

Dipole polarizability

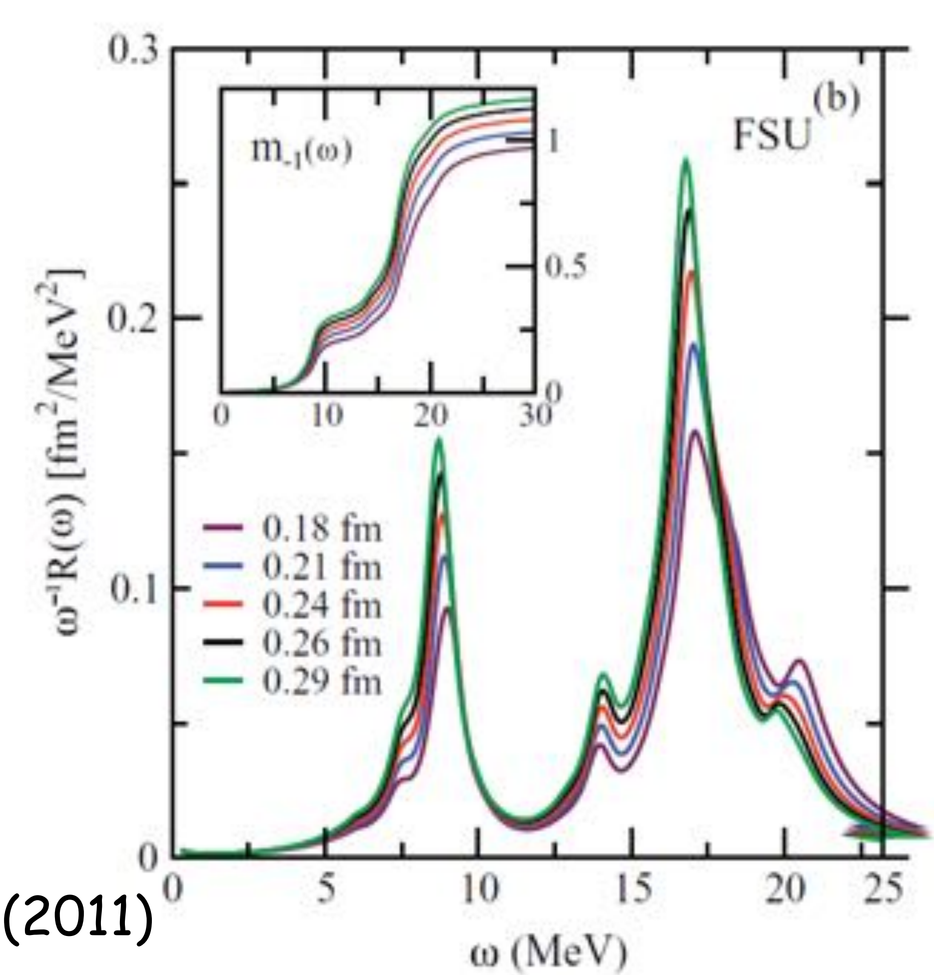

Piekarewicz,
PRC 83, 034319 (2011)

Symmetry energy, neutron skin, and neutron stars

Neutron skin thickness can be obtained from:

(a) elastic proton scattering or coherent photoproduction of neutral pions with well-known charge radii from elastic electron scattering.

(b) antiproton annihilation.

(c) parity-violating elastic electron scattering.

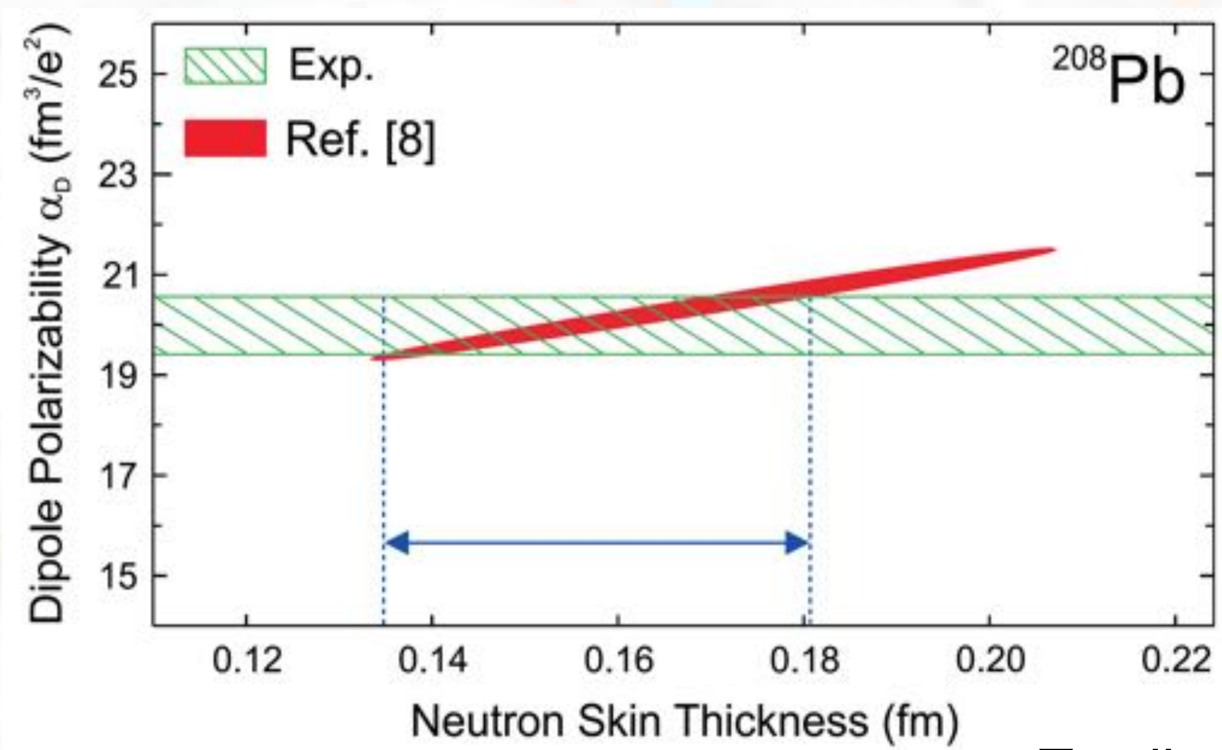

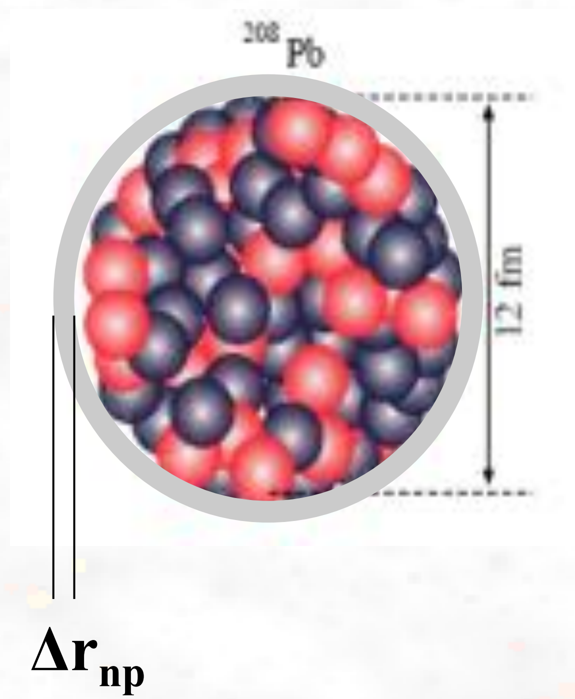

Tamii et al., PRL 107, 062502 (2011)

Nuclear response for PDR, GDR and GQR

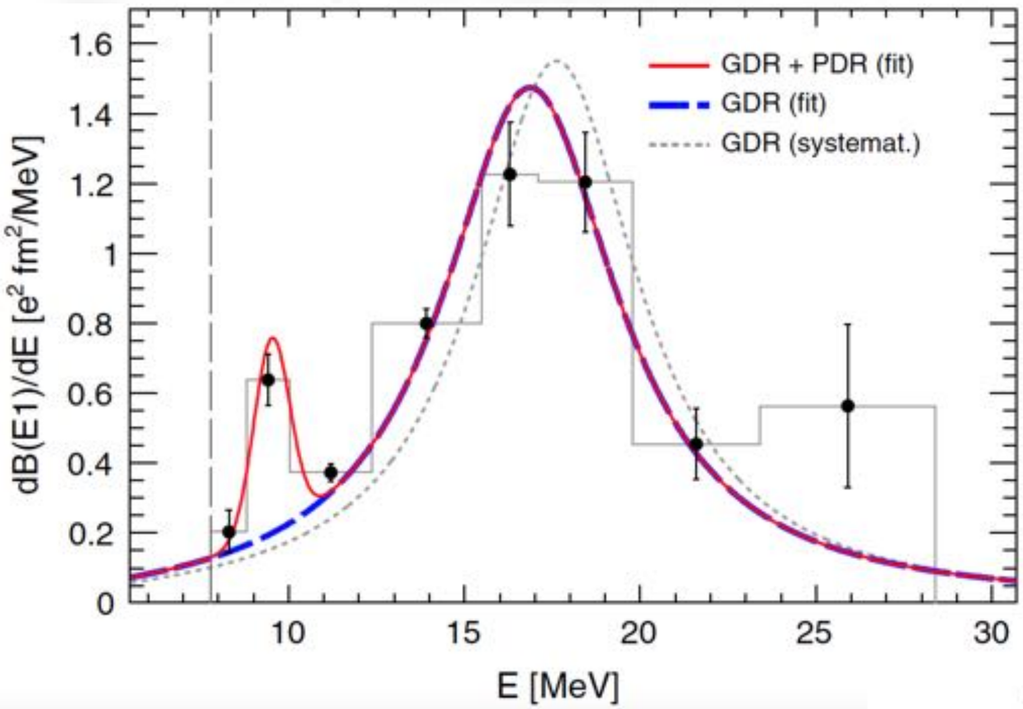

^{68}Ni

Rossi et al.,
PRL 11, 242503 (2013)

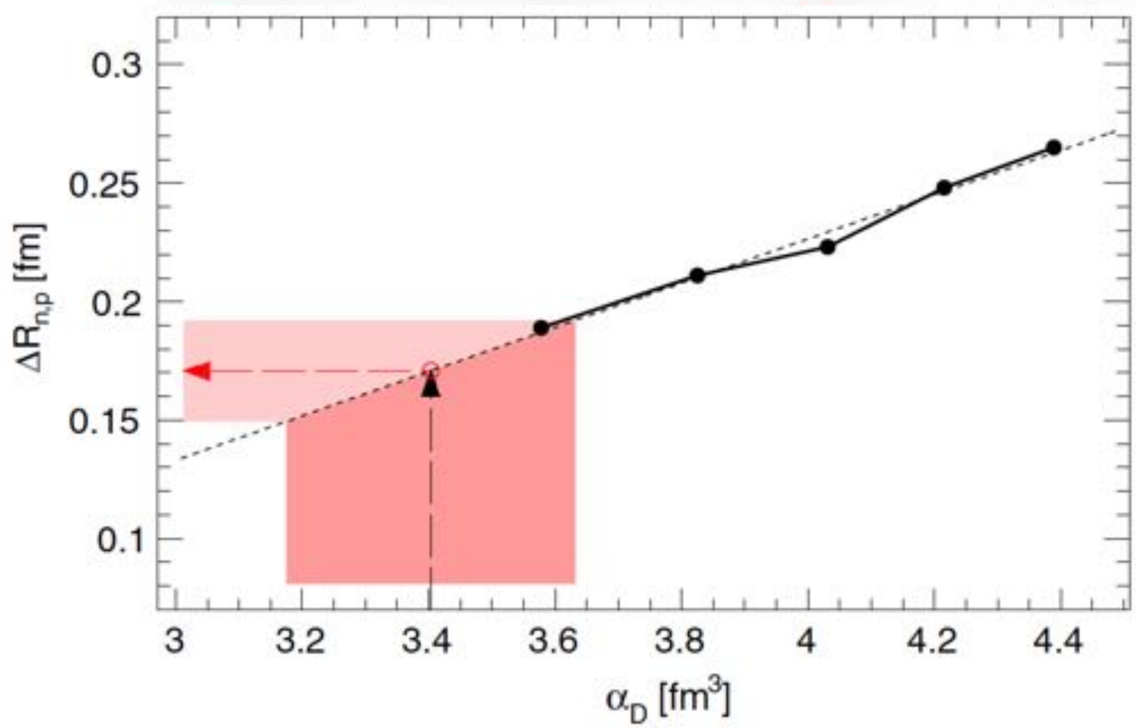

Dynamical coupling of PDR, GDR and GQR

Brady, Aumann, CB, Thomas
Phys. Lett. B 757, 553 (2016)

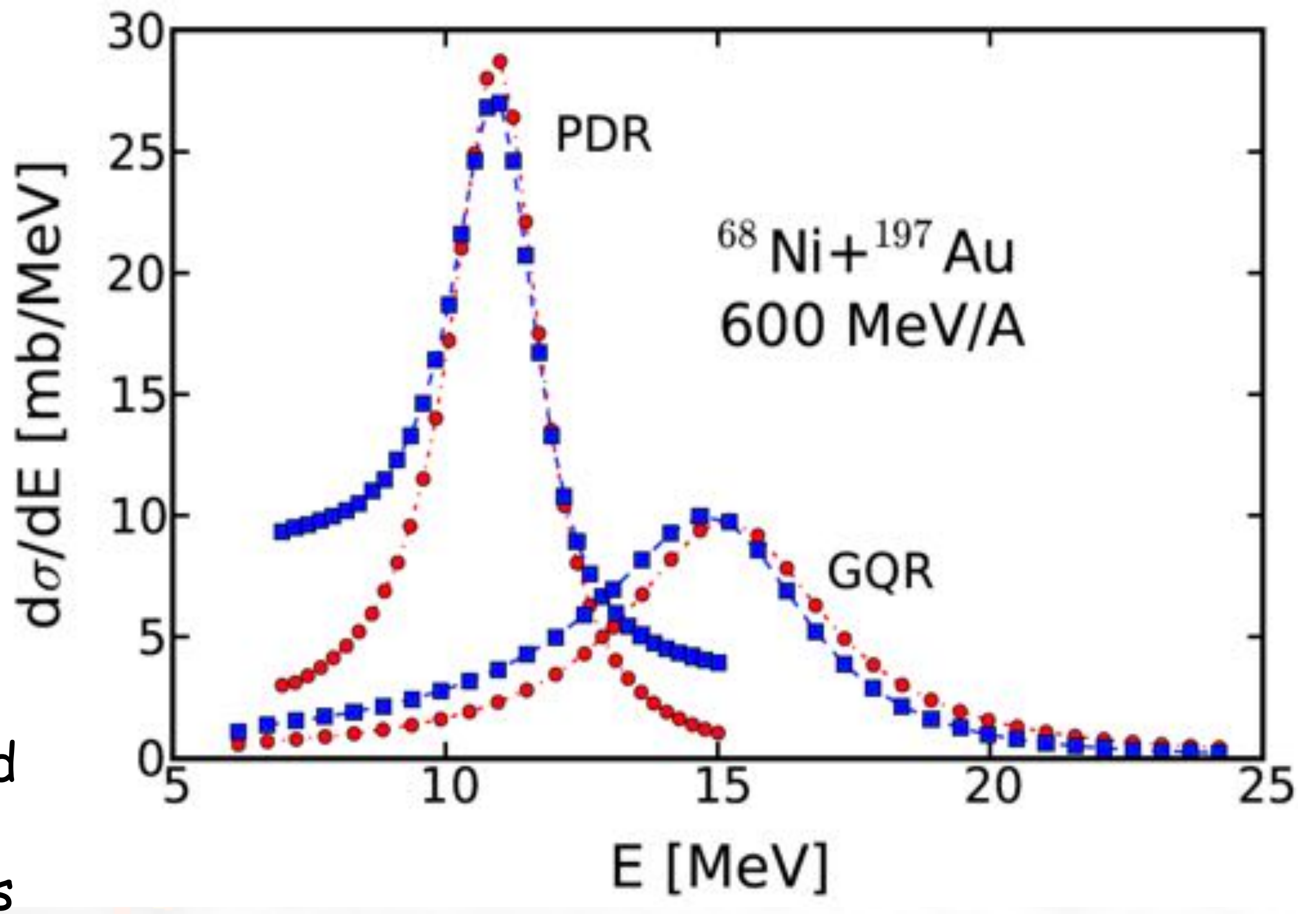

- Nuclear response discretized
- Coupled Channels calculations

●. First order

● all orders relativistic

Dynamical coupling of PDR, GDR and GQR

Brady, Aumann, CB, Thomas
Phys. Lett. B 757, 553 (2016)

- Nuclear response discretized
- Coupled Channels calculations

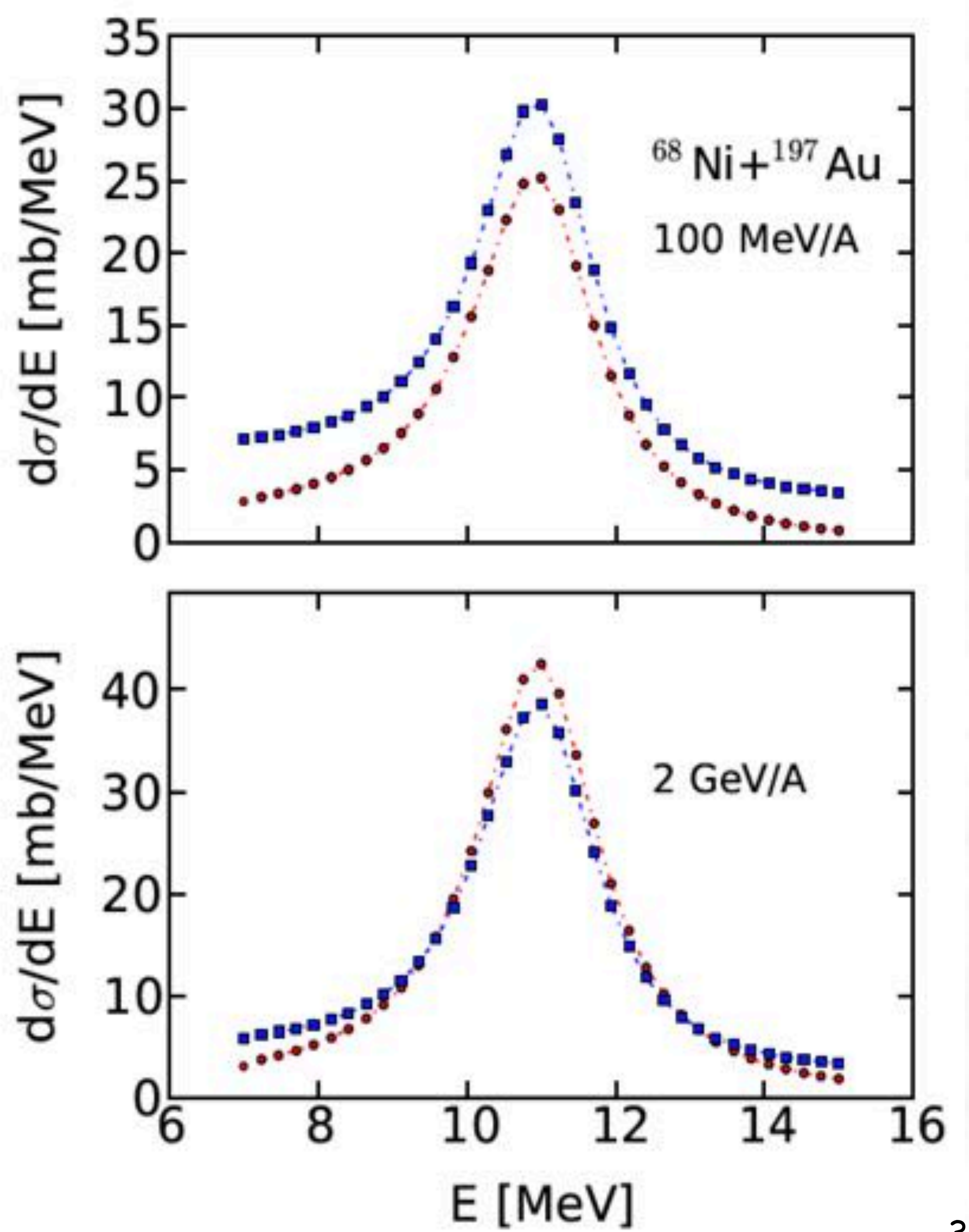

●. First order

● all orders relativistic

Dynamical coupling of PDR, GDR and GQR

Rossi at al.,
PRL 111, 242503 (2013)
→ α_D = 3.40 fm^3

Our new analysis
→ α_D = 3.16 fm^3

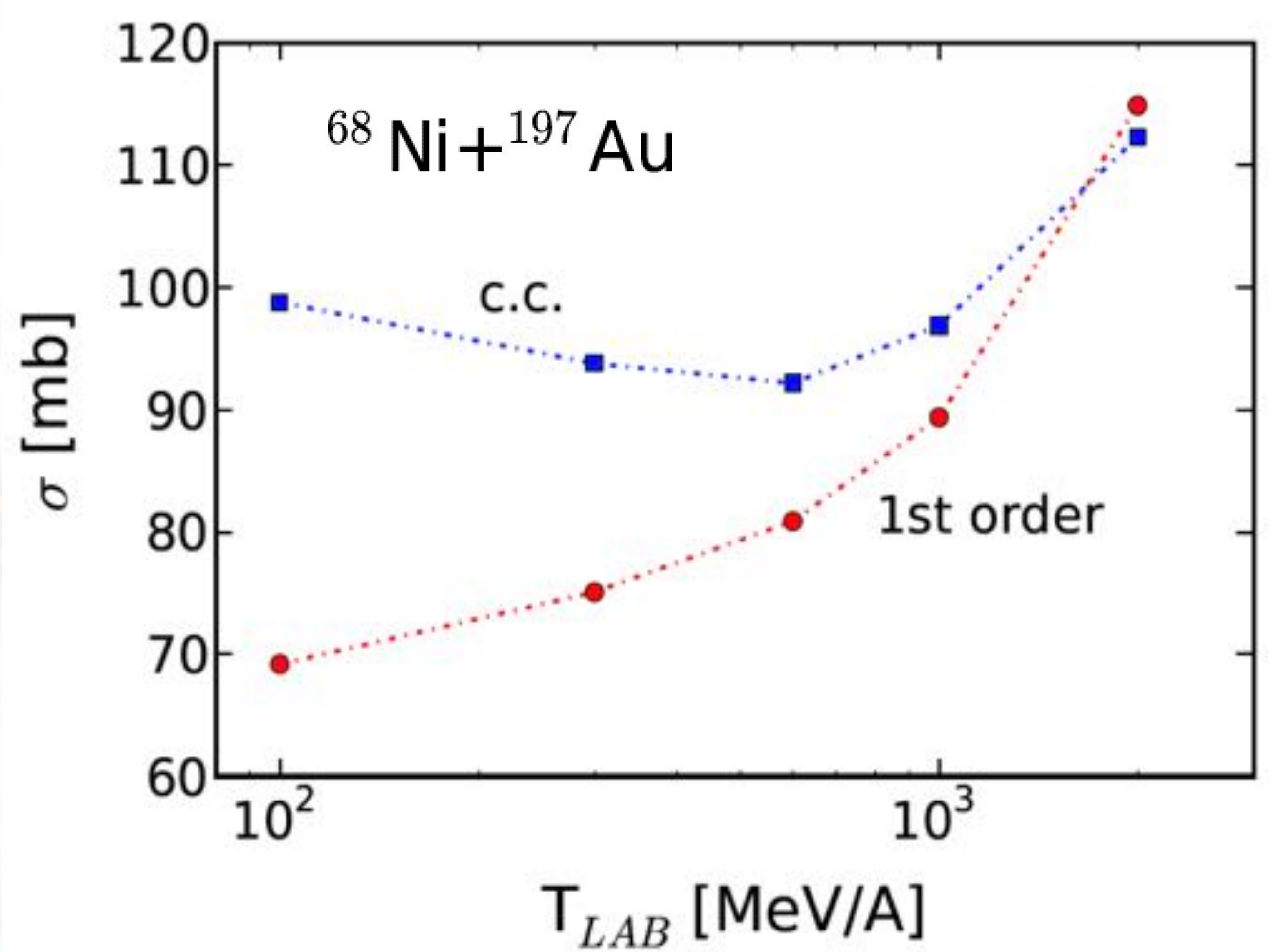

Neutron skin
→ Δr_n = 0.17 fm

Our new analysis
→ Δr_n = 0.16 fm

BUT, experimental error
= 7% for α_D and
= 0.2 for Δr_n

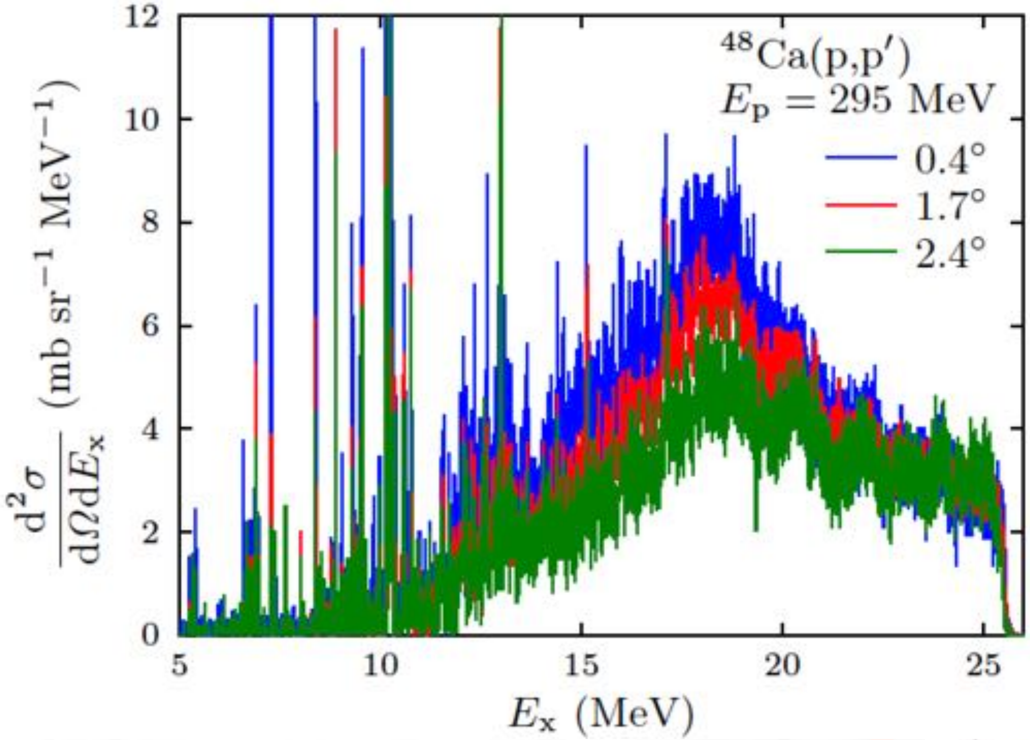

Centroid = 18.9(2) MeV

Width = 3.9(4) MeV

85% sum rule

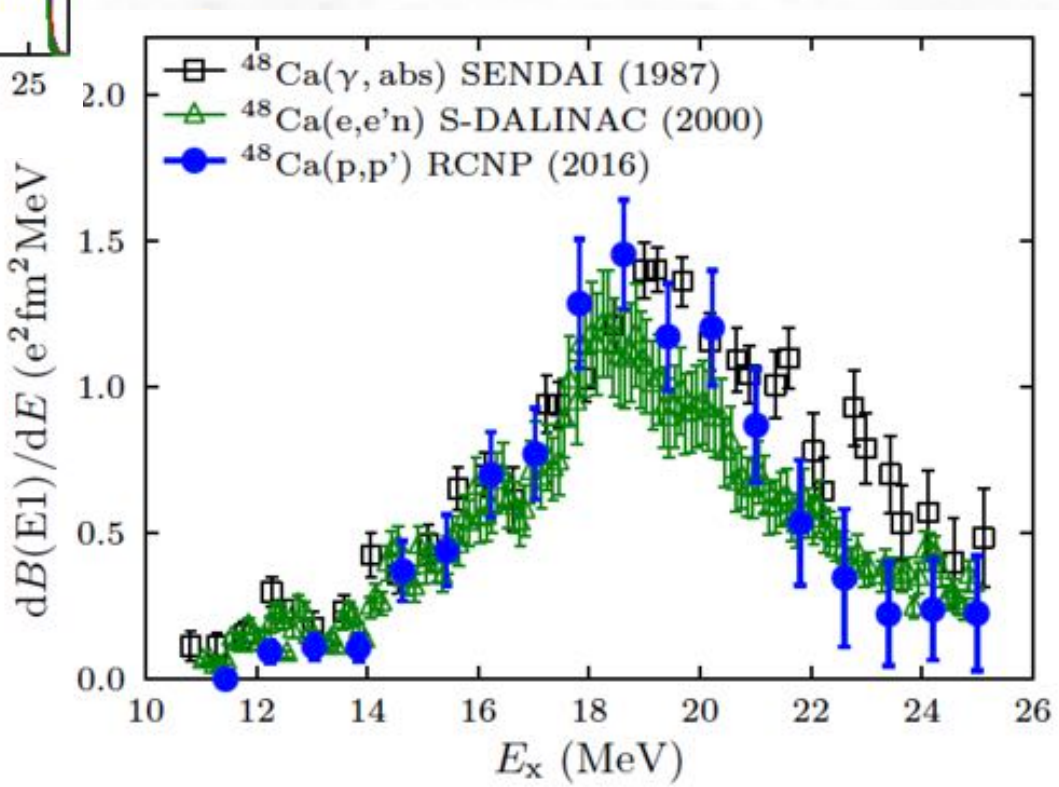

Von Neumann-Cosel & collaborators

PRELIMINARY

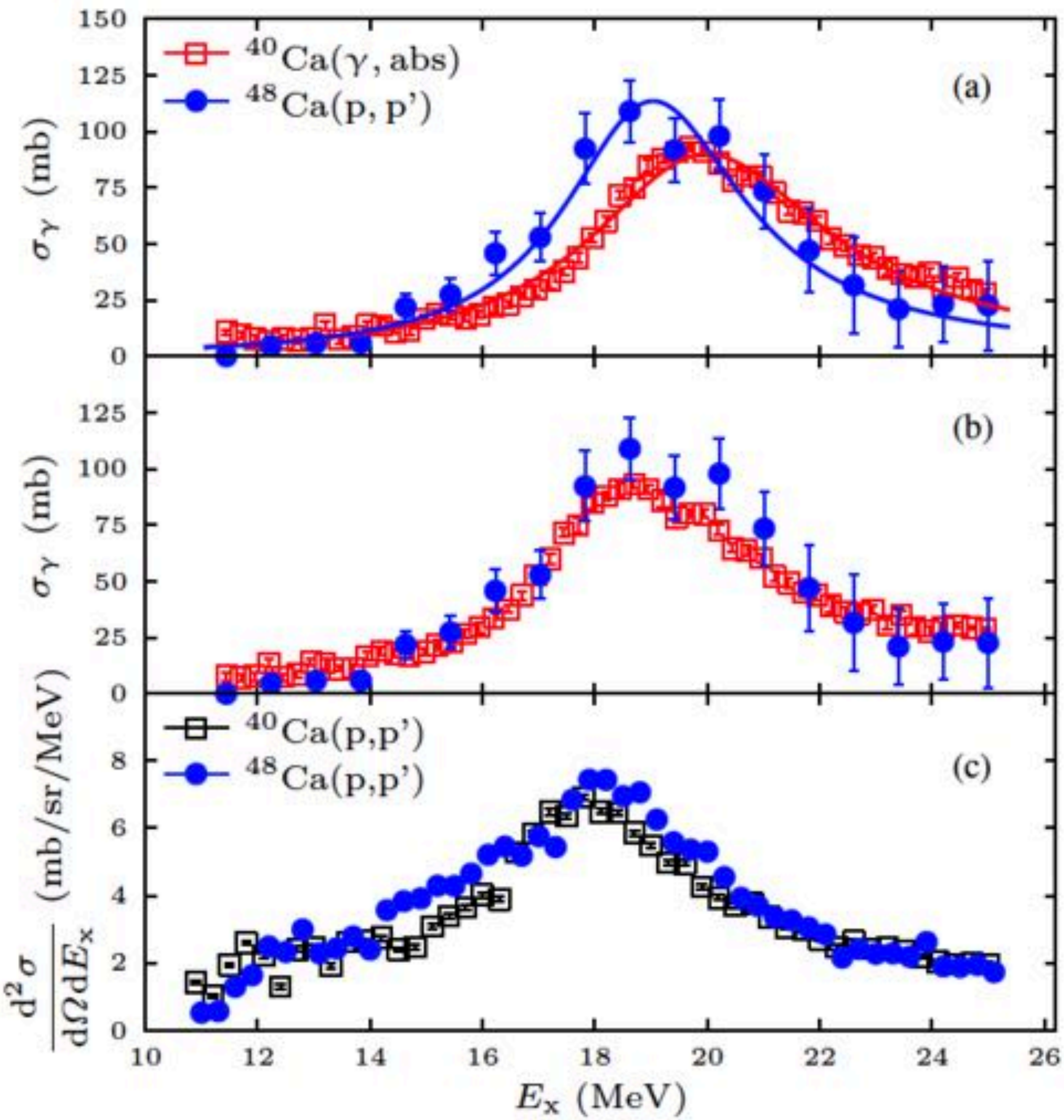

Centroid = 18.9(2) MeV

Width = 3.9(4) MeV

85% sum rule

Von Neumann-Cosel
& collaborators

PRELIMINARY

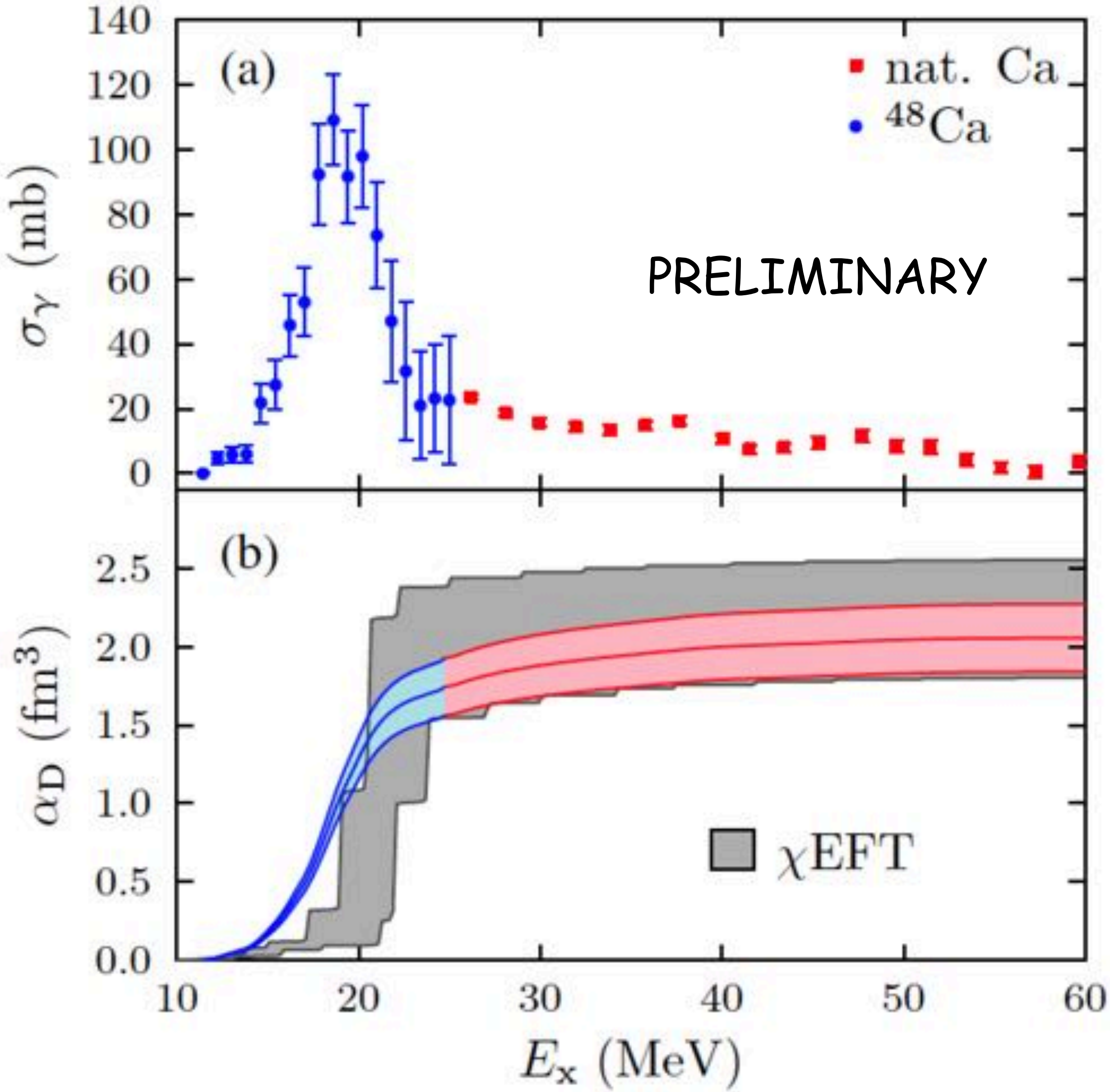

Experiment:

$\alpha_D(^{40}Ca)$ = 1.50(2) fm^3

$\alpha_D(^{48}Ca)$ = 2.07(22) fm^3

Theory:

$\alpha_D(^{40}Ca)$ = 1.87(3) fm^3

Neutron skin:

0.14 – 0.20 fm

PRELIMINARY

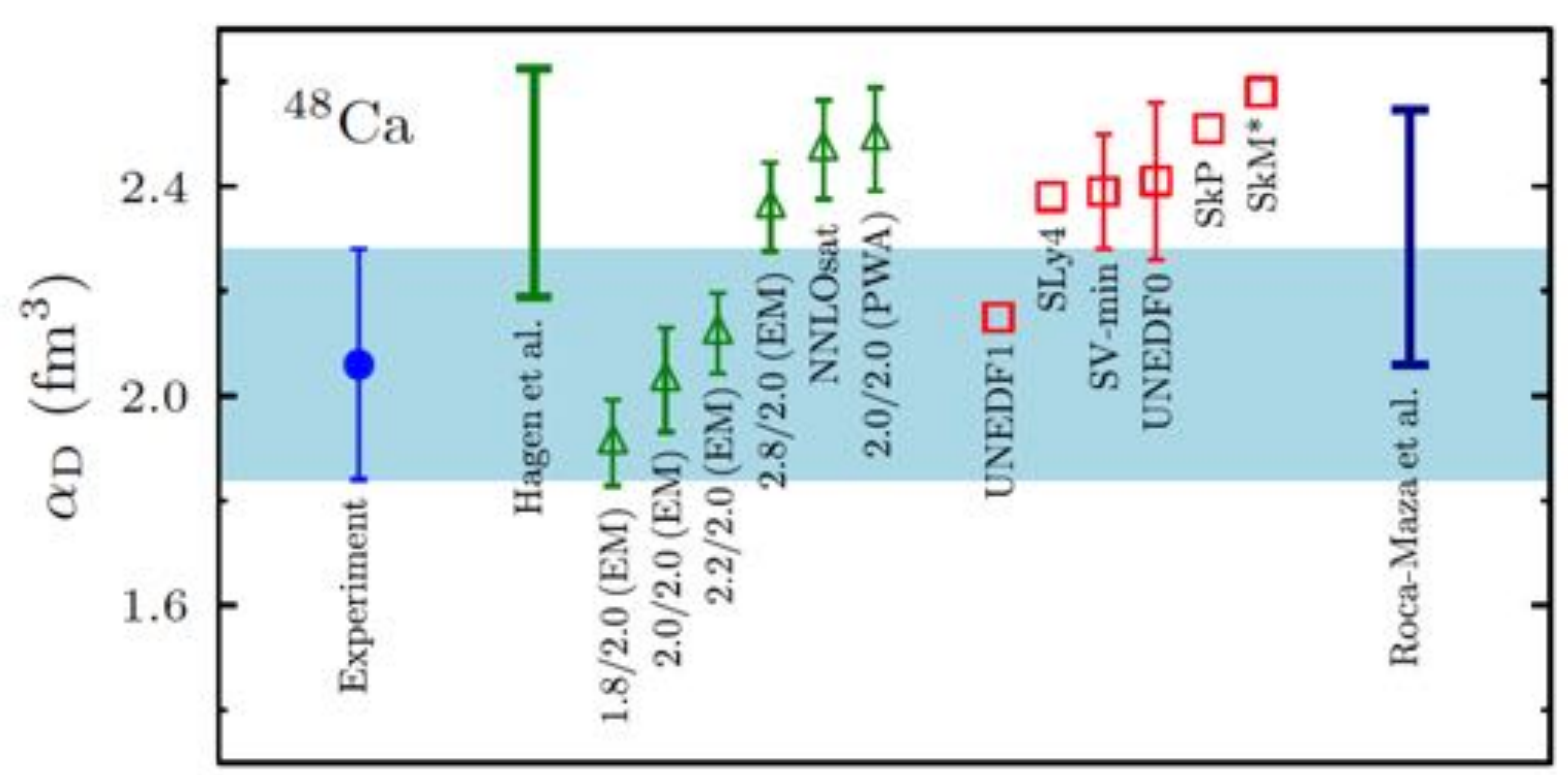

Comparison of the experimental electric dipole polarizability in 48Ca (blue band) with predictions from EFT (green triangles) and χEDFs (red squares)

G. Hagen, A. Ekstr om, G. R. Jansen, W. Nazarewicz, T. Papenbrock, K. A. Wendt, B. Carlsson, C. Forssen, M. Hjorth-Jensen, S. Bacca, et al., Nature Physics 12, 186 (2016).

A. Tamii, I. Poltoratska, P. von Neumann-Cosel, Y. Fujita, T. Adachi, C. A. Bertulani, J. Carter, M. Dozono, H. Fujita, K. Fujita, et al.,
Phys. Rev. Lett. 107, 062502 (2011).

T. Hashimoto, A. M. Krumbholz, P.-G. Reinhard, A. Tamii, P. von Neumann-Cosel, T. Adachi, N. Aoi, C. A. Bertulani, H. Fujita, Y. Fujita, et al.,
Phys. Rev. C 92, 031305 (2015).

I. Poltoratska, P. von Neumann-Cosel, A. Tamii, T. Adachi, C. A. Bertulani, J. Carter, M. Dozono, H. Fujita, K. Fujita, Y. Fujita, et al.,
Phys. Rev. C 85, 041304 (2012).

A. M. Krumbholz, P. von Neumann-Cosel, T. Hashimoto, A. Tamii, T. Adachi, C. Bertulani, H. Fujita, Y. Fujita, E. Ganioglu, K. Hatanaka, et al.,
Phys. Lett. B 744, 7 (2015).

Conclusions

Pairing important for EOS

- Improves masses, binding and odd-even staggering
- But complicates determination of best Skyrme functionals
- Isovector pairing means improvements ← but with additional parameters
- Reasonable description of neutron skins

Pigmy resonances

- Controversial in light nuclei
- Established in medium and heavy nuclei
- Best probed with Coulex – dynamical couplings important
- Extraction of dipole polarizability